Investigation of disease-associated scaffold proteins in the

postsynaptic density

Inaugural-Dissertation

to obtain the academic degree

Doctor rerum naturalium (Dr. rer. nat.)

submitted to the Department of Biology, Chemistry and Pharmacy

of Freie Universität Berlin

by

Hanna Zieger

Berlin, 2019

Die vorliegende Arbeit wurde im Zeitraum von 2014 bis 2018 im Neurowissenschaftlichen Forschungszentrum der Charité-Universitätsmedizin Berlin unter Anleitung von Professor Sarah Shoichet angefertigt.

1. Gutachterin: Professor Sarah Shoichet, NWFZ, Charité-Universitätsmedizin Berlin

2. Gutachterin: Professor Ursula Koch, Freie Universität Berlin

Disputation am: 27. Mai 2019

Danksagung

Content

Index of figures

Index of tables

Declaration on the presentation of published data

Parts of the presented work, including both text and figures, have been published in BioRxiv (Zieger et al., 2019, bioRxiv doi: 10.1101/532374). In this published work, I generated the data shown in all of the figures with assistance from other lab members for specific technical aspects, and I wrote the manuscript text with the assistance of my supervisor. Specifically, parts of figures 6, 7, 8, 13, 14, 15, 16, 17 and 18 and the corresponding text have been published in the manuscript mentioned above.

Summary

Connector Enhancer of Kinase Suppressor of Ras (CNK2) is a disease-associated scaffold protein that is expressed specifically in nervous tissue. Patients with CNK2 mutations exhibit an array of neurocognitive symptoms, ranging from mild intellectual disability (ID) and language delay to more severe and general delayed cognitive and motor development. Seizures are also present in most patients (Damiano et al., 2017; Vaags et al., 2014). Understanding the molecular details of the function of CNK2 during development of nervous tissue will contribute to our knowledge about how CNK2 alterations can cause neurodevelopmental disorders. To explore the function of CNK2, we first examined its specific localisation in cultured rat hippocampal neurons and validated that CNK2 is expressed in neurons and enriched at postsynaptic sites (Iida et al., 2002). We next utilised an shRNA-mediated knockdown approach to explore the effects of loss of CNK2 function at these postsynaptic sites, *i.e.* in dendritic spines of glutamatergic neurons, and observed a reduction in PSD size. Next, we explored the effect of truncated CNK2 variants in neurons. In neurons expressing a disease-associated CNK2 variant (CNK2-P1), we saw an increase in PSD size and a reduced exchange rate in dendritic spines compared to that for wild-type CNK2. We also took advantage of several other CNK2 variants and comparatively investigated their properties in heterologous cells and in dendritic spines. Expression of EGFP-CNK2-ΔPH, a CNK2 variant which lacks the ability to attach to the membrane, caused a reduction in PSD size, which resembles the phenotype we observed in CNK2-knockdown neurons. Further studies revealed a set of novel binding partners for CNK2. Taking advantage of a yeast-two-hybrid approach to screen for brain-expressed CNK2 interaction partners, we identified several binding partners that may participate in the execution of CNK2-mediated regulatory functions in neurons. Interestingly, the proteins identified were not structural proteins that have been previously shown to participate in regulating PSD size. Instead, our list of interacting proteins consisted predominantly of regulatory proteins, including, for example the Rho-GTPase activating protein Vilse/ARHGAP39, which has previously been investigated for its role in mediating CNK2 function (Lim et al., 2014), and the regulatory kinases MINK1

4

and TNIK. Subsequent studies explored the new link between CNK2 and the kinases of the MINK1/TNIK family, for which we discovered a specific interaction with CNK2; these proteins do not interact with CNK1, for example. We focussed specifically on the new CNK2-interacting kinase TNIK, which, like CNK2, was recently implicated in cognitive disorders (Anazi et al., 2016). TNIK is a well-characterised signalling molecule that plays a decisive role in the activation of multiple signal cascades (Larhammar et al., 2017; Wang et al., 2016). More recently, it has been shown that it is concentrated in dendritic spines (Burette et al., 2015), and that it plays a role, together with MINK1, in the regulation of α-amino-3-hydroxy-5-methyl-4-isoxazolepropionic acid (AMPA) receptor trafficking (Hussain et al., 2010). We observed a clear functional interdependency between CNK2 and TNIK: subcellular localisation of TNIK is regulated by CNK2 in heterologous cells and in neurons. We confirmed that CNK2 and TNIK exhibit overlapping expression in dendrites and at postsynaptic sites, and taking advantage of TNIK-binding CNK2 variants that exhibit aberrant subcellular localisation, we demonstrated that CNK2 directly modulates neuronal TNIK, and thus provide strong support for the idea that TNIK and CNK2 participate in common pathways that may be critical for the observed CNK2-mediated regulation of PSD size. In summary, our data provide evidence supporting the idea that CNK2 and TNIK/MINK1 family kinases work together in the neuronal environment to ensure proper development and regulation of dendritic spines.

Zusammenfassung

Connector Enhancer of Kinase Suppressor of Ras2 (CNK2) ist ein krankheits-assoziiertes Gerüstprotein das spezifisch in neuronalem Gewebe exprimiert wird. Patienten, die eine Mutation im CNK2 Gen haben, leiden an einer Reihe neurokognitiver Symptome, die von milder geistiger Behinderung und verzögerter Sprachentwicklung bis hin zu schwerer und weitreichender Verzögerung in der geistigen und motorischen Entwicklung reichen. In manchen Patienten treten auch Krampfanfälle auf (Damiano et al., 2017; Vaags et al., 2014). Ein Verständnis über die molekularen Feinheiten der Funktion von CNK2 während der Entwicklung würde zu unserem Wissen darüber beitragen, wie Veränderungen in CNK2 neuronale Entwicklungsstörungen verursachen können. Um die Funktion von CNK2 zu erforschen, haben wir erst die genaue Lokalisation in kultivierten Neuronen aus dem Hippokampus von Ratten untersucht und bestätigt, dass CNK2 in Neuronen exprimiert und in der Postsynapse angereichert ist. Als nächstes nutzten wir einen shRNA vermittelten knockdown Ansatz, um die Auswirkungen des Funktionsverlustes von CNK2 in der Postsynapse, insbesondere in den dendritischen Dornfortsätzen glutamaterger Neurone, zu untersuchen. Hierbei stellten wir eine Größenminderung der postsynaptischen Dichte fest. Anschließend untersuchten wir die Auswirkung verkürzter CNK2 Varianten in Neuronen. In Neuronen, die die krankheits-assoziierte CNK2 Variante (CNK2-P1) exprimierten, sahen wir eine Vergrößerung der postsynaptischen Dichte und eine geringere Austauschrate im Vergleich zu CNK2 im Wildtyp. Wir nutzten auch mehrere CNK2 Varianten und verglichen ihre Eigenschaften in heterologen Zellen und in dendritischen Dornfortsätzen. Expression von EGFP-CNK2-ΔPH, einer CNK2 Variante die ihre Fähigkeit an die Membran zu binden, verloren hat, verursachte eine Größenminderung der postsynaptischen Dichte, was dem Phänotyp ähnelt, den wir bei CNK2 knockdown beobachten. Anschließende Untersuchungen lieferten eine Reihe neuer Interaktionspartner von CNK2. Wir zogen Nutzen aus der Methode des Hefe-zwei-Hybrid-Systems um nach neuartigen CNK2 Interaktionspartnern zu suchen, die im Gehirn exprimiert sind, und identifizierten mehrere Bindepartner, die an der Ausführung CNK2-vermittelter, regulatorischer

Funktion in Neuronen beteiligt sein könnten. Interessanterweise waren die identifizierten Proteine nicht Strukturproteine, von denen bereits bekannt war, dass sie an der Größenregulierung der PSD beteiligt sind. Stattdessen bestand unsere Liste von interagierenden Proteinen überwiegend aus regulatorischen Proteinen. Darunter zum Beispiel das Rho-GTPase aktivierende Protein Vilse/ARHGAP39, dessen Rolle bei der Funktionsvermittlung von CNK2 schon vorher untersucht wurde (Lim et al., 2014), sowie die regulatorischen Kinasen MINK1 und TNIK. Die folgenden Studien untersuchten den neuen Zusammenhang zwischen CNK2 und den Kinasen der MINK1/TNIK Familie und fanden heraus, dass diese spezifisch mit CNK2 interagieren; diese Proteine interagieren zum Beispiel nicht mit CNK1. Wir fokussierten uns gezielt auf die neue, CNK2-bindende Kinase TNIK, die, genau wie CNK2, kürzlich mit kognitiven Störungen in Verbindung gebracht wurde (Anazi et al., 2016). TNIK ist ein gut-charakterisiertes Signalmolekül, das eine maßgebliche Rolle bei der Aktivierung mehrerer Signalkaskaden spielt (Larhammar et al., 2017; Wang et al., 2016). Erst kürzlich wurde gezeigt, dass es in dendritischen Dornfortsätzen konzentriert ist (Burette et al., 2015), und dass es zusammen mit MINK1 eine Rolle bei der Regulation des Austauschs von AMPA Rezeptoren spielt (Hussain et al., 2010). Wir beobachteten eine eindeutige Wechselbeziehung zwischen CNK2 und TNIK: subzelluläre Lokalisation von TNIK ist in heterologen Zellen sowie in Neuronen von CNK2 reguliert. Wir bestätigten, dass CNK2 und TNIK überschneidende Expression in Dendriten und der Postsynapse aufweisen. Wenn wir uns TNIK-bindende CNK2 Varianten zu Nutze machten, die eine anomale subzelluläre Lokalisation aufweisen, konnten wir zeigen, dass CNK2 neuronales TNIK direkt moduliert, und bieten somit nachdrückliche Unterstützung für die Idee, dass TNIK und CNK2 an gemeinsamen Signalwegen beteiligt sind, die für die beobachtete, CNK2-vermittelte Größenregulierung der PSD kritisch sein könnten.

Zusammenfassend liefern unsere Daten Beweise, die die Idee unterstützen, dass CNK2 und die Kinasen der MINK1/TNIK Familie gemeinsam im neuronalen Umfeld wirken um die einwandfreie Entwicklung und Regulation dendritischer Dornfortsätze zu gewährleisten.

1. Introduction

1.1 Synapses – the connections between neurons

The brain is a highly complex, dynamic and adaptive organ. It processes stimuli from our environment and stores the memories we generate throughout our lives. Neurons are polar cells capable of receiving, integrating and propagating signals. The human brain consists of 86 billion neurons (Herculano-Houzel, 2009; von Bartheld et al., 2016), which are highly connected via synapses, where the transmission between neurons takes place. Every neuron gives rise to one axon, which forms contacts to dendritic spines of other neurons via synapses. Here the propagating, electrical signal is transformed to a chemical one: Vesicles in the presynapse release excitatory (*e.g.* glutamate) or inhibitory (*e.g.* γ - aminobutyric acid (GABA)) neurotransmitters into the synaptic cleft. They are bound by receptors on the postsynaptic side, which are clustered by specialised proteins within the spine. Dendritic spines are actin-rich protrusions – mature spines have a mushroom form - along the dendrites of neurons, which are densely packed with several hundred different proteins organising the synaptic structure and machinery (Collins et al., 2006).

1.2 The postsynaptic density

The postsynaptic density (PSD) is an electron-dense structure at the postsynaptic membrane of a synaptic junction (Gray, 1959). At glutamatergic synapses, these structures have been studied intensely. Although they vary in size and shape, in general PSDs harbour more than 1000 proteins (Bayes et al., 2011; Collins et al., 2006), and these proteins are highly organised and fine-tuned in terms of expression, localisation, interaction and activity (Chen et al., 2018; Collins et al., 2006). These structures are assembled not only of receptor subunits and scaffold proteins, but also include adhesion proteins, ion channels and catalytically active enzymes (Choquet and Triller, 2013; Frank and Grant, 2017). These higher order complexes are capable of reacting to extracellular stimuli; they regulate surface expression, recycling, and trafficking and diffusion of glutamate receptors, and play an important role in synaptic function and plasticity.

Neurotransmitter receptors have to be highly dynamic to encode new information or depending on the activity of the neuron, store memories (Ziv and Fisher-Lavie, 2014). This shift from encoding to storage is organised via interactions with scaffold protein complexes, which are often regulated by phosphorylation (Choquet and Triller, 2013). Multiple studies on various aspects of synapse function and dynamics highlight that the PSD is a protein-dense, fine-tuned network that reacts very sensitively to malfunction of its components.

1.3 Postsynaptic scaffold proteins

Scaffold proteins are multi-domain proteins that typically lack enzymatic activity. They are crucial in regulating signal transduction cascades: scaffold proteins have various domains, which enable interactions with various binding partners. Through protein-protein interactions, scaffold proteins organise protein complex formation and ensure spatiotemporal organisation of signalling processes and signal propagation (Chen et al., 2018; Good et al., 2011; Li et al., 2017). At the postsynapse, scaffold proteins are important regulators of receptor dynamics and synaptic plasticity. They interact with neurotransmitter receptors and are involved in regulating signalling cascades, for example by mediating interactions between catalytically active proteins; this way they fine tune signalling within the synapse (Good et al., 2011; Iasevoli et al., 2013). Synaptic scaffold proteins organise the synapse and provide the structural basis for anchoring neurotransmitter receptors. Several studies provide support for a model in which the PSD is organised in three major scaffold layers, as depicted in the scheme adapted from Sheng and Kim in **Figure 1** (Fernandez et al., 2009; Kim et al., 1997; Li et al., 2017; Naisbitt et al., 1999; Sheng and Kim, 2011; Vinade et al., 2003). The upper layer builds the platform for interaction with glutamate receptors and harbours cell adhesion proteins like Neuroligins, which ensure the connection to the presynapse. This upper layer, most closely associated with the postsynaptic membrane, is also largely composed of membrane-associated guanylate kinase (MAGUK)-family members, including *e. g.* the prototypical postsynaptic scaffold molecule PSD-95 (Fernandez et al., 2009; Vinade et al.,

2003), which are also sometimes referred to as DLGs (disks large guanylate kinases), based on some of the functional traits of a *Drosophila* homologue. An intermediate layer, composed of disk large associated guanylate-associated proteins (DLGAPs) that are also referred to as GKAPs because of their ability to bind GK domains. At the PSD, GKAPs bind to the GK domain of members of the PSD-95 family like PSD-95, PSD-93, SAP97 and SAP102, and link clusters of glutamate receptors and PSD-95 to the downstream signalling components (Kim et al., 1997). The lower scaffold layer consists of SH3 and multiple Ankyrin repeat domains protein (SHANK)-family scaffold proteins (Naisbitt et al., 1999). Together with Homer, SHANK proteins build the network of scaffold proteins that sits deeper in the PSD (Sheng and Kim, 2011). Via its interaction with GKAP, SHANK is connected to PSD-95 and glutamate receptors on the one side and mediates downstream signalling and contact with the actin cytoskeleton on the other (Sheng and Kim, 2011). Mutations in more than 100 postsynaptic scaffold proteins (Bayes et al., 2011; Laumonnier et al., 2007) have been associated with brain disorders; malfunction or mislocalisation of these proteins can have drastic effects on proper synapse development and synaptic transmission (Iasevoli et al., 2013; MacLaren et al., 2011).
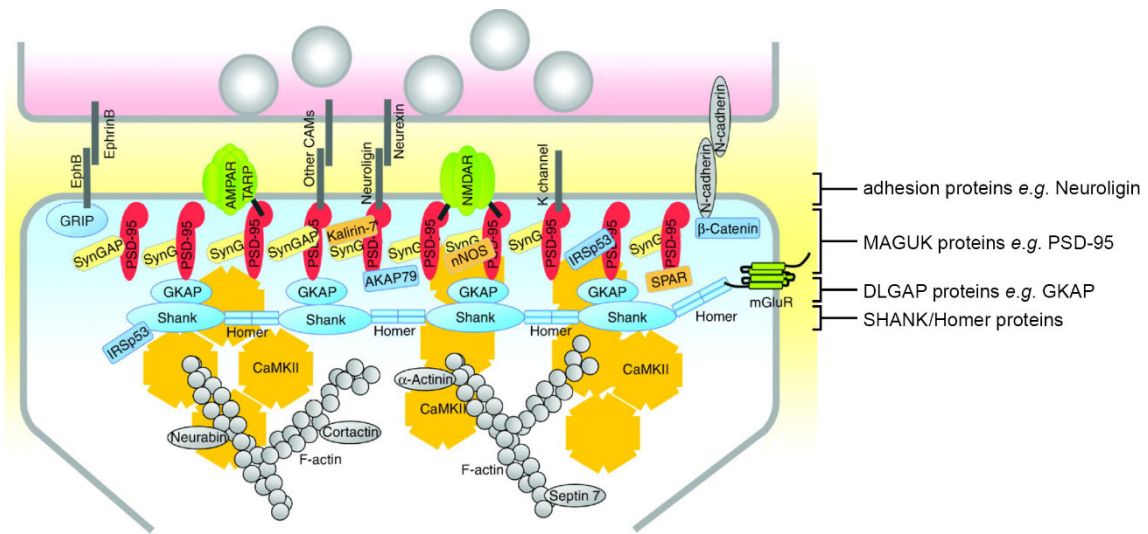
Figure 1: Scheme of the PSD of an excitatory postsynapse

Members of the MAGUK family *e. g.* PSD-95 sit close to the postsynaptic membrane, DLGAP/GKAPs are part of the intermediate scaffold layer, and the lower layer consists of SHANK and Homer scaffolds. Contact and overlap of illustrated proteins indicates interaction.
Image adapted from Sheng and Kim, 2011.

1.4 The CNK scaffold protein family

1.4.1 The scaffold protein CNK is conserved

In this study, the central focus is on the scaffold protein called Connector Enhancer of Kinase Suppressor of Ras (CNK/CNKSR), which was originally identified through its functional association with KSR scaffold proteins in the regulation of upstream modulators of Mitogen-Activated Protein Kinase (MAPK) pathways (for an overview, see (Claperon and Therrien, 2007)). MAPK pathways are protein kinase cascades activated by an extracellular mitogen binding to a membrane receptor. This allows small GTPases (*e. g.* Ras) to exchange their bound GDP by GTP and activate their downstream target MAPKKK (*e. g.* RAF) by phosphorylation, which in turn phosphorylates MAPKK, which then phosphorylates MAPK. MAPK can now activate a transcription factor and this way reacts to external stimuli (*e. g.* stress signals) by modulating gene expression. Scaffold proteins *e. g.* KSRs have various roles in signalling pathways and are required for efficient signalling: they physically assemble the individual kinases of the MAPK cascades

(including upstream regulators), regulate MAPK localisation (*e. g.* membrane association of protein kinases) and they can segregate MAPK signalling proteins from competing inputs (*e. g.* components from different MAPK pathways) (Good et al., 2011; Morrison and Davis, 2003).

The scaffold protein CNK/CNKSR was first discovered in *Drosophila*, where it was shown to regulate Ras/MAPK signalling by binding to the Ras effector RAF (Claperon and Therrien, 2007; Douziech et al., 2003; Therrien et al., 1998) and thereby play an essential role in eye and wing development (Lanigan et al., 2003; Therrien et al., 1998). The GTPase Ras functions as a molecular switch controlling intracellular signalling networks and thereby regulates processes such as cell proliferation, migration and actin cytoskeletal integrity (Schoneborn et al., 2018; Wennerberg et al., 2005). In neurons, expression of constitutively active Rap2 (a Ras family member) results in spine loss and dendrite retraction, whereas constitutively active Ras induces outgrowth of dendritic spines (Stornetta and Zhu, 2011).

Subsequent studies on CNKs in various organisms showed that CNK homologues are present across species, ranging *e. g.* from *C. elegans* (Rocheleau et al., 2005) to humans (Lanigan et al., 2003). In humans, there are three homologues present: CNK1, CNK2 and CNK3 (Lim et al., 2010). CNKs possess various protein interaction domains, including *e. g.* a sterile alpha motif (SAM), a conserved region in CNK (CRIC), a PSD-95/DLG-1/ZO-1 (PDZ) domain, proline-rich motifs, and a pleckstrin homology (PH) domain (see **Fig. 4**), and the domain architecture is essentially conserved throughout the CNK family proteins and also across species. SAM domains interact with SAM domains of other proteins (Qiao and Bowie, 2005), PDZ domains bind to PDZ ligands *e. g.* the cytosolic termini of glutamate receptors (Kim and Sheng, 2004), proline-rich motifs specifically bind to WW and SH3 domains (Macias et al., 2002), and PH domains bind to phosphatidylinositol lipids in biological membranes (Lemmon, 2008).

In *Drosophila,* CNK influences signalling by acting as a scaffold downstream of the GTPase Ras, as well as in the Ral pathway, which suggests a role for CNK in integrating

signals between the Rlf and the MAPK pathways (Lanigan et al., 2003). Since the original discovery of the D-CNK protein in *Drosophila*, it has become clear that CNK family homologues serve as scaffolds for multiple signal cascades. By interacting with various guanine nucleotide exchange factors (GEFs) and GTPase activating proteins (GAPs), they modulate signalling mediated not only by Ras but also via Rho family small GTPases (Jaffe et al., 2004; Jaffe et al., 2005; Lim et al., 2014; Lim et al., 2010). It has further been shown that CNKs interact with the Cytohesin family of ArfGEFs. The Sec7 domain of Cytohesins promote the replacement of GDP with GTP, which activates the GTPases ARF1, ARF3, ARF5 and ARF6. CNKs facilitate the membrane recruitment of Cytohesins, and thereby regulate *e. g.* the insulin signalling pathway (Lim et al., 2014; Lim et al., 2010). Other studies suggest that CNKs may also regulate cell proliferation and migration by acting as scaffolds directly for the PI3K/Akt pathway (Fritz et al., 2010) and the JNK (MAPK) signalling cascades (Cho et al., 2014). It has further been shown that CNKs act as positive feedback regulators of the RAF/MAPKK/ERK pathway and are involved in cell proliferation and migration depending of their membrane localisation (Fischer et al., 2017; Wolfstetter et al., 2017).

1.4.2 CNK2 in neurons

Among the known CNK proteins, mammalian CNK2, also known as CNKSR2 or MAGUIN (membrane-associated guanylate kinase-interacting protein) has various isoforms. CNK2a (MAGUIN-1) and CNK2b (MAGUIN-2) exhibit tissue-specific expression in nervous tissue (Yao et al., 1999) where they are concentrated at the postsynaptic sites of neurons (Iida et al., 2002). There are two studies suggesting a role for CNK2 in neuronal morphology. In one study, the authors explored the effect of loss of CNK2 in mouse hippocampal neurons and could show that shRNA-mediated knockdown of CNK2 resulted in reduced total neurite length, reduced number of branches, and reduced branching complexity. These phenotypes could be rescued by expression of knockdown-resistant CNK2 (Hu et al., 2016). In another study, the authors

identified the GTPase activating protein (GAP) Vilse/ArhGAP39 (Lim et al., 2014) as a novel interaction partner of CNK2 using mass spectrometry. The authors provided evidence supporting a role for CNK2 in regulating GTPase activity in neurons (Lim et al., 2014) and also showed that lack of CNK2 abolished spine maturation (Lim et al., 2014). Other studies have focussed on how CNK2 isoforms participate in protein-protein interactions (Bumeister et al., 2004). Previously identified CNK2 interaction partners include, for example, the scaffold proteins PSD-95 and S-SCAM (Yao et al., 1999), as well as Densin-180 (Ohtakara et al., 2002), which is associated with N-methyl-D-aspartate (NMDA) receptors and metabotropic glutamate receptors. A recent high-throughput study suggests that CNK2 may be part of the core scaffold machinery that assembles synaptic signalling complexes in the PSD during development (Li et al., 2017).

1.4.3 CNK2 is disease associated

Relatively few studies focus specifically on the scaffold function of CNK2 in neurons and in the brain (Lim et al., 2014; Ohtakara et al., 2002), despite an increasing number of genetic studies that directly implicate CNK2 mutations in human brain disorders (Aypar et al., 2015; Damiano et al., 2017; Houge et al., 2012; Hu et al., 2016; Najmabadi et al., 2011; Sun et al., 2018; Vaags et al., 2014). CNK2 is a disease-associated scaffold protein that is expressed specifically in nervous tissue. Cnk2 lies on chromosome Xp22.12 and is associated with X-linked intellectual disability (XLID). Genes associated with psychiatric and neurological conditions are distributed throughout the human genome. However, compared to the autosomes, many more genes influencing cognitive function have been found on the X-chromosome (Laumonnier et al., 2007; Ropers and Hamel, 2005; Skuse, 2005). In cases of intellectual disability ~20 % more males than females are affected, and in numerous families, ID is inherited in an X-linked pattern (Laumonnier et al., 2007). In females, one copy of the X-chromosome is inactivated and the unaffected X-chromosome can in theory compensate for an X-linked mutation. For this reason, in most familial cases described, the mothers are unaffected carriers or exhibited only a mild learning disability in childhood. When CNK2 is lacking due to copy number variation (CNV) or nonsense

mutation, the affected male patients are intellectually disabled, delayed in their cognitive and motor development and have a highly restricted speech; in some cases, an abrupt life-long loss of language is described. Further symptoms are attention deficits, hyperactivity and early childhood epilepsy. In most patients, the seizures respond to medication. Some patients showed continuous spike-and-slow-waves (CSWS), disappearing in patients older than 10 years; others show symptoms of epilepsy aphasia syndrome (EAS) (Aypar et al., 2015; Damiano et al., 2017; Houge et al., 2012; Hu et al., 2016; Najmabadi et al., 2011; Sun et al., 2018; Vaags et al., 2014). Together, these reports suggest that CNK2 plays a key role during neurodevelopment, which provided the motivation for this project. Here we have investigated the function of the scaffold protein CNK2, with the aim to contribute to our molecular understanding of the role of CNK2 in neurons, thereby contributing to our knowledge about disease pathology in patients with CNK2 defects.

2. Materials and Methods

2.1 Materials

2.1.1 Bacteria

Table 1: Escherichia coli

Bacteria	Origin	Supplier
E. coli	OneShot Top10	Invitrogen

2.1.2 Cell Culture

Table 2: Cell line

Cell line	Origin	Supplier
COS-7	Cercopithecus aethiops, kidney cells	ATCC

Table 3: Reagents for Cell Culture

Reagent	Working concentration
Collagen (3.36 mg/ml)	50 µg/ml 0.02% acetic acid
Poly-D-Lysin, Sigma (10mg/ml)	0,2 mg/ml PBS
Laminin, Sigma (1mg/ml)	2 µg/ml PBS
B27 Supplement 50x, Gibco	1x
L-Glutamin 200mM, Lonza	0.5 mM
Neurobasalmedium, Gibco	
DMEM, Lonza	
Trypsin-EDTA Mixture	
PBS (sterile), Lonza	
FBS Superior, Biochrom	

Table 4: Media for Cell Culture

Cell type	Composition
COS-7	DMEM, 10% FCS, PEN-STREP (1000U/ml), 2mM L-Glutamine
primary rat hippocampal neurons	Neurobasalmedium, 1x B27-Supplement, 0,5mM L-Glutamine

2.1.3 Oligonucleotides

Table 5: Oligonucleotides

Primer name	Sequence
Cnk2-SalI-fw	aagtcgacatggctctgataatggaaccgg
Cnk2-BamHI-rv	ttggatccttagcttttctctccaac
Cnk2ΔPH-rv	ttggatccttagccaagatcctttca
Cnk2ΔDUF-PH-rv	ttggatccttaaagcatgctctgagg
Cnk2ΔPDZ-DUF-PH-rv	ttggatccttattccaggtgagcaga
Cnk2-P1-rv	aaggatcctcatgggtatgtgtcatag
Cnk2-P2-rv	aaggatccttatttcttgtgactgaatagtcttgtcac
Cnk2-NotI-fw	aagcggccgcatggctctgataatggaa
Cnk2-KpnI-rv	ttggtaccgcttttctctccaacgtt
rCnk1NotI-fw	aagcggccgcatggagcccgtggag
rCnk1-BglII-rv	aaagatctgggaggtcaggaggtt
Mink1-C-XbaI-fw	aatctagaatgcagcagaactctccc
Mink1-rv	gtaaccattataagctgc

2.1.4 Antibodies

Table 6: Primary antibodies

Antibody	Host	Company
anti-CNK2	guinea pig	Eurogentec (custom-made)
anti-CNK2	rabbit	Sigma/Atlas (HPA 001502)
anti-HOMER-1	guinea pig	Synaptic Systems (160004)
anti-MAP2	guinea pig	Synaptic Systems (188004)
anti-MAP2	mouse	Millipore (05-346)
anti-Mortalin	mouse	Antibodies Inc. (75-127)
anti-PSD-95	mouse	Antibodies Inc. (75-028)
anti-Synapsin-1	rabbit	Synaptic systems (106 103)
anti-TNIK	mouse	Santa Cruz (sc-136103)
anti-FLAG-HRP	mouse	Sigma (A8592)
anti-GFP	chicken	Abcam (ab139708)
anti-GFP	mouse	Roche (11814460001)
anti-GFP	goat	Abcam (ab6673)
anti-V5	mouse	Invitrogen (R960-25)
anti-V5	rabbit	Millipore (AB3792)
normal IgG	mouse	Santa Cruz (sc-2025)

Table 7: Secondary antibodies

Antibody	Company
anti-mouse-HRP	Dianova, (115-035-003)
anti-rabbit-HRP	Dianova (111-035-003)
anti-goat-HRP	Santa Cruz (sc-2020)
anti-guinea pig Alexa Fluor 405	Abcam (ab175678)
anti-mouse Alexa Fluor 405	Invitrogen (A-31553)
anti-guinea pig Alexa Fluor 488	ThermoFisher (A-11073)
anti-chicken Alexa Fluor 488	Jackson Immuno Research (703-545-155)
anti-rabbit Alexa Fluor 568	Life Technologies (A-11036)

| anti-mouse Alexa Fluor 568 | Life Technologies (A-11031) |

2.1.5 Reagents

Table 8: Reagents

Reagent	Supplier
Acetic acid	Merck
Acrylamide	Roth
Agar-agar	Roth
Agarose	Serva
Ammonium persulfate (APS)	Biomol
Ampicillin	Roth
ß-mercaptoethanol	Roth
bis-tris free base	Sigma
BSA	Sigma
Complete mini protease inhibitors	Roche
DMEM (1 g/l Glucose) (sterile)	Lonza
DMEM low Glucose	Sigma
dNTPs	Perkin Elmer
DPBS (sterile)	Lonza
DTT	AppliChem
EDTA	Merck
Ethidium bromide (1% solution)	Roth
FastDigest green buffer	Fermentas
FBS	Biochrom
Fluoromount-G	Southern Biotech
Dapi-Fluoromount -G	Southern Biotech
Glycerol	Merck
Glycine	Merck
HCl	Roth

Isopropanol	Merck
Kanamycin (-sulfate)	Roth
KCl	Merck
KH2PO4	Roth
L-glutamine	Lonza
Lipofectamine2000	Invitrogen
Methanol	Merck
Na2HPO4	Roth
NaCl	Merck
NaOH	Roth
Nuclease free water	Ambion
Opti-MEM	Gibco
Paraformaldehyde (PFA)	Merck
PCR reagents (DMSO, MgCl2,10x PCR Buffer)	NEB
Penicillin-streptomycin (10.000 U)	Lonza
Phusion Hi-Fi DNA Polymerase	NEB
Poly-L-lysine	Sigma
Powdered milk	Roth
all Restriction enzymes	MBI Fermentas (Fast Digest)
SDS	Roth
TEMED	Roth
Tris	Merck
Triton X-100	Sigma
Tryptone	Fluka
Tween20	Sigma
Western Lightning	Perkin Elmer
Xylene cyanol	Sigma
Yeast extract	Roth
Zeocin	Invitrogen

2.1.6 Buffers and Solutions

Table 9: Composition of Buffers and Solutions

Buffer/ Solution	Composition
1x PBS (pH 7.3) non-sterile	137 mM NaCl
	2.7 mM KCl
	10 mM Na2HPO4
	1.8 mM KH2PO4
PBST	PBS + 0.1% Tween 20
blocking solution (WB)	PBST, 5% milk powder (w/v)
blocking solution (IF)	PBS, 4% BSA (w/v)
4x SDS sample buffer	8% SDS
	40 % Glycerol
	0.25 M Tris pH 6.8
	0.004% Bromophenol Blue
	20 % β-mercaptoethanol
5x Lämmli Buffer	0,25 M Tris
	1.92 M Glycin
	1 % SDS
5x blotting buffer	250 mM Tris
	1.92 M Glycin
1x blotting puffer	+ 10% Methanol
50x TAE	2 M Tris (pH 8.8)
	50 mM EDTA
	5.71 % Acetic Acid
IP lysis buffer	50 mM Tris (pH 7.4)
	100 mM NaCl
	1% TritonX-100
10xDNA loading buffer	23 mM Xylene Cyanol
	18.7 mM Bromphenol Blue
	21.7 mM SDS
	8.6 M Glycerol
LB-medium (pH 7)	0.5% (w/v) yeast extract
	1% (w/v) Trypton
	0.17 M NaCl
LB agar plates	1.5% (w/v) agar in LB-medium
Separating buffer	1.5M Tris pH 8.8
	0.4% SDS
Stacking buffer	1 M Tris pH 6.8
	0.8% SDS

ECS solution	25 mM Hepes (pH 7.4) 140 mM NaCl 1.3 mM CaCl2 5.4 mM KCl 33 mM Glucose

2.1.7 Equipment

Table 10: Consumables

Consumables	Supplier
Blot paper	BioRad
Coverslips, 18mm	VWR
PVDF Membrane	BioRad
Centrifuges (5430 R, 5418 R)	Eppendorf
Centrifuge (Varifuge 3.0R, Biofuge PrimoR	Thermo Scientific
Confocal microscope sp5	Leica
Digital developing system (Chemiluminescence)	GE Healthcare
Spinning Disc Confocal CSU-X	Nikon
Semi-dry blotting system	BioRad
Thermocycler	MJ research/ Bio-Rad
Thermomixer compact	Eppendorf
Vertical electrophoresis system	BioRad

Table 11: Kits

Kits	Supplier (Name)
Gel extraction kit	QIAGEN (QIAquick Gel Extraction Kit)
PCR purification kit	QIAGEN (QIAquick PCR Purification Kit)
Plasmid mini preparation kit	QIAGEN (QIAprep Spin Miniprep Kit)
Plasmid maxi preparation kit	QIAGEN (QIAprep Spin Maxiprep Kit)

2.2 Methods

Expression constructs were PCR amplified using the Phusion Hi-Fi DNA Polymerase and the PCR reagent from New England Biolabs under the PCR thermocycling conditions below.

Table 12: PCR thermocycling conditions

Step	Temperature	Time
Initial Denaturation	98°C	30 seconds
	98°C	5-10 seconds
25-35 Cycles	45-72°C	10-30 seconds
	72°C	15-30 seconds/kb
Final Extension	72°C	5-10 minutes
Hold	4°C	

2.2.1 Expression Constructs

Cnk2 (Accession number: NM_177751) was amplified from cDNA generated from mouse brain by S.-A. Kunde. The pEGFP-C1-Cnk2 construct (accession number: XM_011247826.1) was cloned using the primers Cnk2-SalI-fw and Cnk2-BamHI-rv. For the truncated variants, the forward primer Cnk2-SalI-fw was used together with Cnk2ΔPH-rv for pEGFP-C1 CNK2ΔPH, Cnk2ΔDUF-PH-rv for pEGFP-C1-CNK2ΔDUF-PH, Cnk2ΔPDZ-DUF-PH-rv for pEGFP-C1-CNK2ΔPDZ-DUF-PH, Cnk2-P1-rv for pEGFP-C1-CNK2-P1 and Cnk2-P2-rv for pEGFP-C1-CNK2-P2. PCR products were cloned into pEGFP-C1 (Clontech) using BamHI and SalI restriction sites. EGFP-CNK2 and the truncated variants CNK2ΔPH and CNK2-P1 were cloned into a lentiviral shuttle vector under the control of a human Synapsin-1 promoter using BamHI and SalI restriction sites. Lentivirus was produced by the Viral Core Facilty, Charité Universitätsmedizin Berlin. The vector used is the lentiviral shuttle vector FUGW (Lois et al., 2002), with a human SynapsinI promotor instead of the original promotor and a multiple cloning site inserted. Mouse Cnk2 was subcloned into pBudCE4.1

(Invitrogen) using pBud-Cnk2-Notl-fw and pBud-Cnk2-KpnI-rv. Rat Cnk1 (accession number: BC099788) was amplified from a cDNA-clone (Clone ID: 7934518, Source Bioscience) and subcloned into pBudCE4.1 using the primers rCnk1NotI-fw and rCnk1-BglII-rv.

The CNK2 shRNA (Lim et al., 2014) we used to specifically knockdown CNK2 targeting both rat and mouse CNK2 sequences, was: UGAUUCAGCUGGCAAAUAU, nucleotides 644-662. For CNK2 knockdown in heterologous cells the targeting sequence was cloned into psuper (OligoEngine). For knockdown control, shRNA targeting Renilla Luciferase cloned by N. Rademacher into psuper was used. For knockdown in neurons we used a lentiviral vector with a nuclear localized RFP expression, a human RNA-polymerase-III-promotor U6 controlling the transcription of the shRNA and a human SynapsinI promotor controlling the expression in neurons. Scrambled Clathrin shRNA was used as knockdown control.

Vectors expressing FLAG-TNIK and FLAG-MINK1 were generous gifts from Natasha Hussain, (Hussain et al, 2011). FLAG MINK1-C (AA 534-1310) was subcloned using the primers Mink1-C-XbaI-fw and Mink1-rv.

2.2.2 Co-immunoprecipitation, SDS-PAGE and western blot

COS-7 cells were maintained in DMEM (Lonza) supplemented with 10 % FBS (Sigma), 2 mM L- glutamine and penicillin/streptomycin at 37 °C with 5 % CO_2. Transient transfections were done using Lipofectamine 2000 (Invitrogen) according to the manufacturer's recommendations. Transfected COS-7 cells (T75 flask) were harvested 18-20 hours post transfection in PBS (pH 7.4) using a cell scraper and pelleted by centrifugation at 1200 x g. COS-7 cell pellets were lysed in 1 ml lysis buffer (50 mM Tris (pH 7.5), 100 mM NaCl, 1% Triton X) and lysed using a 30G needle. Lysates (1 ml) were cleared by two centrifugations for 10 min at 20817 x g and incubated with the appropriate antibody for 3 hours at 4°C. Lysates were cleared by centrifugation for 10 min at 20817 x g. Supernatants were incubated with 30 µl Protein G-Agarose (Roche) per ml lysate for 1 hour at 4 °C and washed three times with lysis buffer. Immunocomplexes were collected

by centrifugation, denatured, and analysed by SDS-PAGE and western blot (semi-dry blotting system, Bio-Rad). PVDF-membranes (Bio-Rad) were blocked (PBS, 0.1 % Tween 20, 5 % dry milk) and incubated overnight with primary antibody. Membranes were incubated for 1 hour at 4 °C with the respective horseradish peroxidase (HRP)-conjugated secondary antibody. If the primary antibody used was conjugated to HRP no secondary antibody was added. Western Lightning Plus-ECL was used to visualise the signal on the blot and recorded with Image Quant (LAS4000Mini, GE Healthcare). To detect other proteins of interest on the same membrane, the membrane was incubated overnight at 4°C in blocking buffer containing 0.1 % sodium azide with subsequent primary and secondary antibody as described before. For coIP from cultured neurons, infected neurons were washed with warm PBS, subsequently lysed in lysis buffer and further treated as described above.

2.2.3 Immunofluorescence COS-7 cells

For immunofluorescence COS-7 cells on glass coverslips, coated with Collagen, were washed with PBS 18-20 hours post transfection and fixed in 4 % PFA in PBS for 10 min. After washing with PBS, the cells were permeabilised in 0.2 % Triton-X in PBS for 5 min, washed again with PBS and blocked with 4 % bovine serum albumin (BSA) in PBS for 1 h at room temperature. Cells were incubated with primary antibodies in 4% BSA in PBS at 4 °C overnight, washed with PBS and subsequently incubated with secondary antibodies in blocking solution for 1 h. After washes in PBS, coverslips were dipped in deionized water and mounted with Dapi-Fluoromount-G or Fluoromount-G (Southern Biotech).

2.2.4 Neuron culture

For primary rat hippocampal neuronal cultures, embryonic E18 Wistar rats were used. Following decapitation, hippocampi from embryos were isolated and collected in ice-cold DMEM (Lonza). Neurons were separated using Trypsin/EDTA (Lonza) at 37 °C for 5 min. After stopping the reaction with 10 % FBS (Biochrom) in DMEM and subsequent washing in DMEM to remove trypsin, the hippocampal tissue was suspended in neuron

culture medium (Neurobasal supplemented with B27 and 0.5 mM glutamine) and further dissociated mechanically. For immunofluorescence, neurons were plated onto glass coverslips (d=18 mm) coated with a mixture of poly-D-lysine (Sigma) and Laminin (Sigma) in PBS at a density of 1.5×10^5 cells per 12-well. For lysates, plates were coated as described before and cells were plated at a density of 7.5×10^5 cells per 6 well. Cell debris was removed after healthy neurons adhered (50 minutes post-plating), and neurons were maintained at 37 °C with 5% CO2 in neuron culture medium.

2.2.5 Lenti-viral infection and Immunofluorescence

Cultured neurons on glass coverslips were infected at DIV3 with lentivirus transducing CNK2 shRNA/ control shRNA and at DIV10 for expression of EGFP, EGFP-CNK2 or EGFP-CNK2ΔPH. At DIV23-24, neurons were fixed in 4 % PFA in PBS for 10 min. After washing with PBS, the cells were permeabilised in 0.2 % Triton-X in PBS for 5 min, washed again with PBS and blocked with 4 % bovine serum albumin (BSA) in PBS for 1 h at room temperature. Cells were incubated with primary antibodies in 4% BSA in PBS at 4 °C overnight, washed with PBS and subsequently incubated with secondary antibodies in blocking solution. After washes in PBS, coverslips were dipped in deionized water and mounted with Fluoromount-G (Southern Biotech).

2.2.6 Imaging

Samples were blinded and randomised before imaging. Images were acquired with a Leica laser-scanning confocal microscope (Leica TCS-SP5 II) provided by the NWFZ Microscopy Core Facility using the 63x immersion oil objective. Total z-stack range of 2 μm was set with a 0.4 μm inter-stack interval and used in a maximal z-stack projection for further analysis.

2.2.7 Fluorescence Recovery After Photobleaching (FRAP)

Fluorescence recovery after photobleaching is a powerful life cell imaging technique to explore mobility and exchange rate of fluorescent (most commonly EGFP-tagged) proteins (Ciocanel et al., 2017; Lippincott-Schwartz et al., 2018; Veerapathiran and

Wohland, 2018). A self-defined region of interest (ROI) is defined in the sample and exposed to a powerful laser pulse. The bleaching causes an irreversible loss of fluorescence in the defined area. Subsequently the recovery of fluorescence in the area bleached is measured over time using a microscope. With this technique exchange rate and mobility of bleached (non-fluorescent) protein and not bleached (still fluorescent) protein can be assessed.

Cultured rat hippocampal neurons were infected at DIV 10 with lentivirus transducing EGFP-CNK2 or EGFP-CNK2-P1. At DIV23-24 medium was supplemented with warm ECS solution before recording. For image acquisition neurons were blinded and randomised and kept in a recording chamber at 37° C and 5% CO2. Images were acquired with a Nikon Spinning Disc Confocal CSU-X microscope from the Advanced Medical Bioimaging Core Facility (AMBIO) of the Charité. Live cell images were taken with a 60x immersion oil objective and a laser with 488 nm wavelength was used. For each neuron imaged, circular regions of interest (ROIs) were defined around spines along the dendrites as depicted in **Figure 2**.
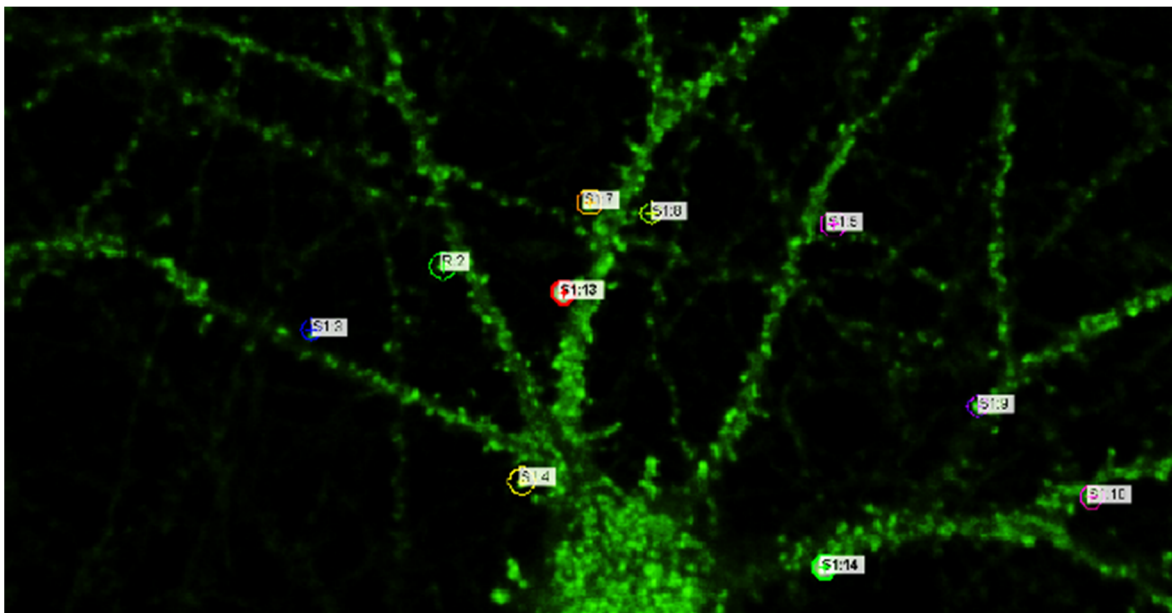
Figure 2: FRAP - Example image

Screenshot of a neuron expressing EGFP-CNK2 with dendritic spines defined as ROIs (coloured circles)
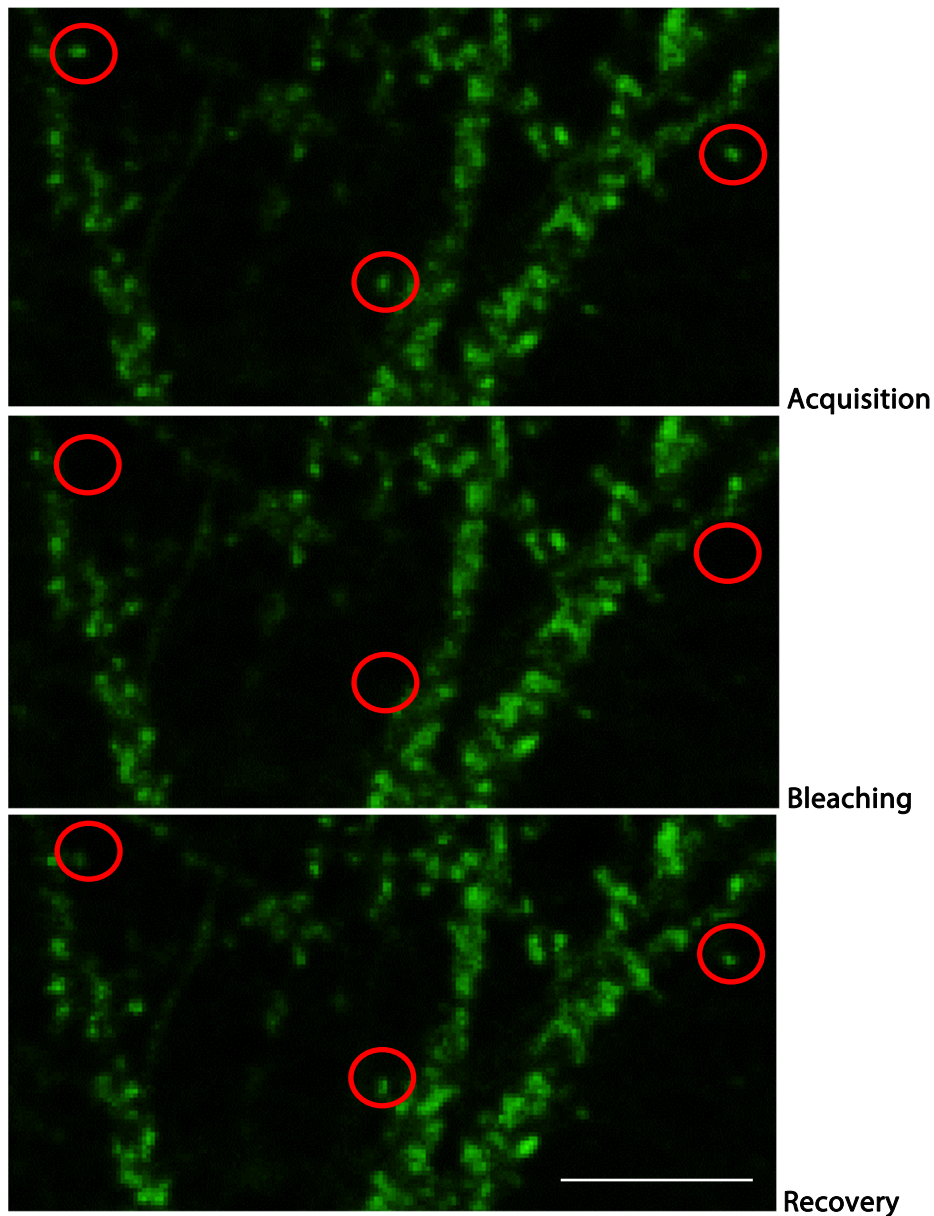
Figure 3: Example images at different timepoints during image acquisition

Acqisition: First image of the baseline; red cirles mark defined ROIs to be bleached. Bleaching: Image taken immedeately after photobleaching. Recovery: Image taken 600 seconds after photobleaching; Fluorescence recovered within the ROIs. Scale bar: 10µm.

The protocol in the table below **(Table 13)** was used for FRAP experiments. Within the defined ROIs a baseline of ten images was taken **(Fig. 3, upper panel)**, followed by 20 loops with the laser (wavelength: 488 nm) at 100% power and a dwell time of 100 µs to bleach the fluorescent (EGFP) signal **(Fig. 3, middle panel)**. After bleaching fluorescence recovery was measured **(Fig. 3, lower panel)**; details about the duration can be found in **Table 13**. Fluorescence intensity was normalised to the mean of the baseline.

Table 13: Protocol for photobleaching and image-acquisition

	Interval	Duration	Loops
Acquisition	No Delay		10
Bleaching	No Delay		20
Acquisition	3 sec	57 sec	20
Acqusition	30 sec	9 min	18

2.2.8 Image Analysis

Analysis was done randomised using FIJI/ ImageJ software (Version 1.52g) (Schindelin et al., 2012). For determination of distribution of EGFP-CNK2 and EGFP-CNK2ΔPH (cyan) and its effect on TNIK (magenta), regions of interest (ROI) were defined along secondary dendrites, 4-6 ROIs per neuron. Fluorescence intensity per ROI was measured for all channels. Intensity for EGFP and TNIK signal was normalised to intensity of MAP2 signal (grey, 405) per ROI. Measured EGFP signal intensity of EGFP-CNK2 and EGFP-CNK2ΔPH was normalised to the mean of EGFP-CNK2 signal. For TNIK distribution, every value was normalised to the mean of TNIK in the control situation (EGFP only). For spine analysis, dendrites were imaged as described before. PSD size, represented by the signal of the postsynaptic marker protein Homer was analysed using the "Analyze Particles" tool of FIJI. For each experiment, the threshold for the Homer staining representing the PSD size was set according to experimenters´ discretion. Every spine measured was normalised to the mean Homer area of the control condition (EGFP).

2.2.9 Crude synaptosome preparation

For the crude synaptosome preparation, cultured neurons were treated with Syn-PER Synaptic Protein Extraction Reagent (Thermo Scientific) according to the manufacturer's recommendations. Neurons lysate was centrifuged at 1200 x g for 10 minutes at 4°C to pellet the nuclei and heavy fragments. The supernatant from the first centrifugation step was centrifuged at 150000 x g for 20 minutes at 4°C to separate the synaptosomes (pellet)

from the cytosolic fraction (supernatant). The different fractions were collected and analysed by SDS-PAGE and western blot.

2.2.10   Custom-made CNK2 antibody

The custom-made CNK2 antibody used in this study was produced by Eurogentec. It was raised in guinea pig against a KHL-conjugated peptide representing CNK2 amino-acids 727-741 (see protein scheme **Fig. 4**) and affinity matrix purified. The peptide is present in all known CNK2 isoforms.

2.2.11   Yeast-Two-Hybrid

The Yeast-Two-Hybrid (Y2H) screen (Hybrigenics ULTImate Y2H) was performed by HYBRIGENICS (Paris, France), using full-length CNK2 (mus musculus, Gene ID: 245684, aa 1-1032), cloned into pB27 (N-LexA-bait-C fusion) with an adult mouse brain cDNA library. The Y2H screen is a very efficient and sensitive method to identify protein interactions and is based on the reconstitution of a functional transcription factor (TF), when two proteins or polypeptides of interest interact. The bait (full length CNK2) is fused to the Gal4 DNA Binding Domain (DBD) and the prey, which are proteins fragments from a library is fused to the Gal4 Activation Domain (AD). Physical binding of the protein of interest to a protein fragment from an adult mouse brain library brings the DBD of the Transcription Factor in close proximity to its AD. This reconstitution of the functional transcription factor upstream of the reporter gene enables transcription of the HIS3 reporter gene. This allows genetically modified yeast strains to selectively grow on medium lacking histidine. New interaction partners can be identified by sequencing the DNA of the positive clones.

3. Results

Mutations in the membrane-associated scaffold protein CNK2 cause developmental disorders; specifically, both deletions (Aypar et al., 2015; Houge et al., 2012; Hu et al., 2016; Najmabadi et al., 2011) and point mutations (Damiano et al., 2017; Sun et al., 2018; Vaags et al., 2014) that result in loss of function of CNK2 cause X-linked intellectual disability (XLID) that is typically associated with seizures. As CNK2 has its highest expression levels in the brain (Yao et al., 1999) (see also www.proteinatlas.org), we were interested particularly in the role of the protein in the development and function of neurons.

3.1 CNK2 is a membrane-associated protein expressed in neurons and enriched at postsynaptic sites

To investigate endogenous CNK2 in neurons, we needed a specific antibody detecting all known isoforms of the protein. As the commercially available antibodies did not meet our expectations, we decided to produce a custom-made antibody together with Eurogentec. The epitope sequence we chose is present in all known CNK2 isoforms. The antibody was raised in guinea pig against a KHL-conjugated peptide representing CNK2 amino-acids 727-741 **(Fig. 4)**.

Figure 4: Scheme of CNK2 showing the epitope sequence

Scheme of CNK2. Domain arcitecture (SAM, sterile alpha motif; CRIC, conserved region in CNK; PDZ, PSD-95/DLG-1/ ZO-1; DUF1170, domain of unknown function; PH, pleckstrin homology). The position of the epitope sequence of the custom made antibody is marked in magenta.

The antibody was tested in immunofluorescence experiments on heterologous cells expressing EGFP-CNK2 and we were happy to see that overexpressed CNK2 was detected by the antibody (**Fig. 5**). We next explored the subcellular localisation of CNK2 and observed a striking membrane-specific localisation of CNK2 **(Fig. 5)**.
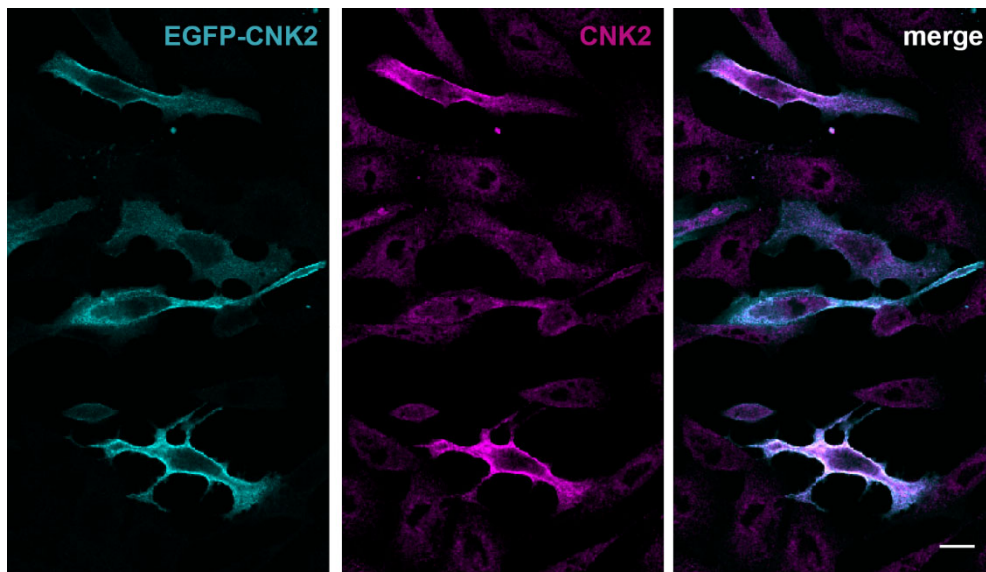
Figure 5: CNK2 is a membrane associated protein

Immunofluorescence experiments on COS-7 cells overexpressing EGFP-CNK2 (cyan) demonstrates that the custom-made CNK2 antibody (magenta) detects CNK2. The staining exhibits membrane localisation of CNK2. Scale bar: 10 μm

From immunofluorescence experiments on cultured primary rat hippocampal neurons at DIV21 we could see that endogenous CNK2 is expressed in neurons **(Fig. 6A)** and is enriched at postsynaptic sites in dendritic spines: it co-localises with PSD-95 **(Fig. 6C)** and shows adjacent staining with the presynaptic marker Synapsin **(Fig. 6D)** (Zieger et al., 2019). The postsynaptic localisation of CNK2 was also observed using other methods: following virus-mediated expression of EGFP-tagged CNK2 in hippocampal neurons, we assessed EGFP signal in mature neurons (DIV21): again, we observed enriched signal intensity in punctate structures along MAP2 positive dendrites **(Fig. 6B)** (Zieger et al., 2019).
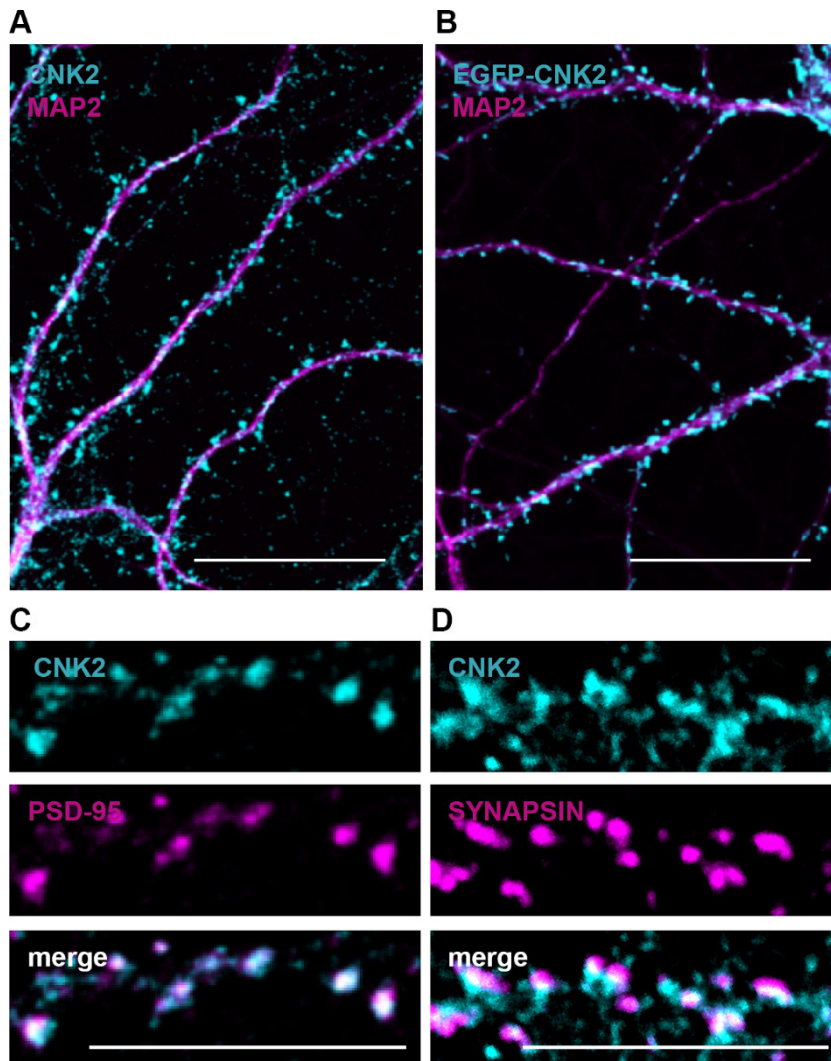
Figure 6: CNK2 is localised in the postsynapse of neurons

(A) Localisation of endogenous CNK2 (cyan) and the dendritic marker MAP2 (magenta) in cultured rat hippocampal neurons (DIV21). Endogenous CNK2 is localised in punctate structures along the dendrite. Scale bar: 20 µm. (B) Localisation of EGFP-CNK2 (cyan) following lentiviral transduction, and the dendritic marker MAP2 (magenta) in cultured rat hippocampal neurons (DIV21). Scale bar 20 µm. (C) CNK2 (cyan) co-localises with post-synaptic marker PSD-95 (magenta). (D) CNK2 (cyan) shows adjacent staining with the presynaptic marker Synapsin (magenta). Scale bar: 10 µm.

3.2 Loss of CNK2 influences the size of the postsynaptic density

Given that loss of CNK2 is implicated in brain disorders, together with our observation that CNK2 is expressed in neurons, in particular in dendrites and at postsynaptic sites, we were interested to explore the idea that dendritic spines might be affected by loss of CNK2. We used an shRNA-mediated knockdown of CNK2 and first tested its efficiency by co-expressing CNK2-V5 with a CNK2 knockdown or a Renilla Luciferase knockdown as control knockdown **(Fig. 7A)**. In order to explore the consequences of CNK2 knockdown in neurons we first assessed the temporal expression of CNK2 in nervous tissue. Based on western blot of mouse brain lysates, we could show that the protein is expressed from postnatal day zero (P0) throughout adulthood **(Fig. 7B)**. We took advantage of lentivirus-

mediated gene delivery of an shRNA to specifically knockdown endogenous CNK2 (Lim et al., 2014) in primary neurons early in development. For these experiments, scrambled Clathrin shRNA was used as control knockdown. We infected cultured neurons at DIV3, and 18-19 days after transduction, crude synaptosomes were prepared and analysed by western blot **(Fig. 7C)**.
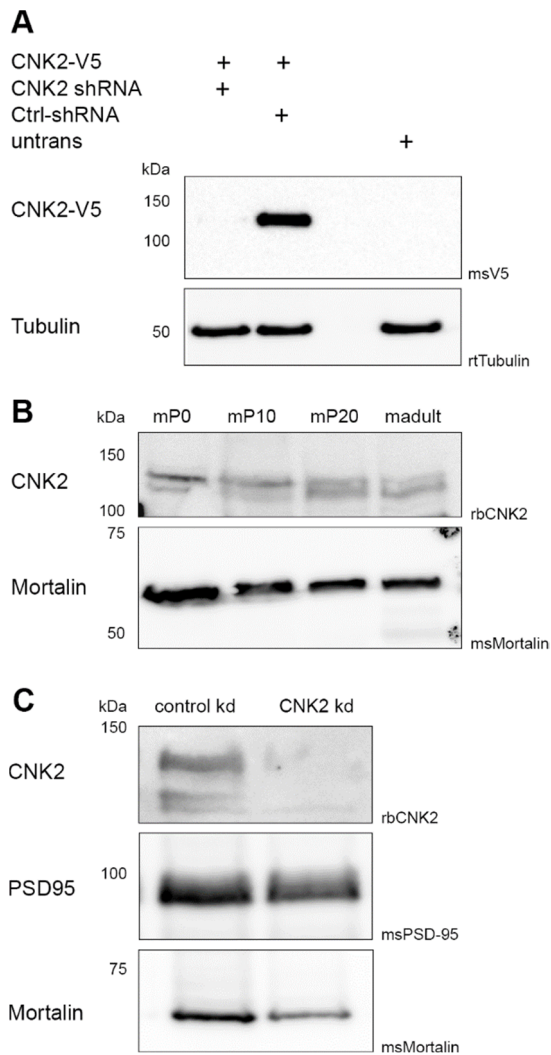
Figure 7: shRNA mediated knockdown of CNK2

(A) Western blot of shRNA mediated knockdown of V5 tagged CNK2 expressed in COS-7 cells. Western blot was probed with rabbit anti-V5 antibody. Tubulin serves as loading control. (B) CNK2 is expressed from P0 throughout adulthood in the mouse brain. Whole cell lysates generated from mouse brains at P0, P10, P20 and adult stage were analysed by SDS-PAGE and western blot with anti-CNK2 antibody. Mortalin serves as loading control (expected size 60 kDa). (C) Synaptosome preparation of primary neurons (DIV23) infected with lentivirus transducing shRNA (DIV3) to knockdown endogenous CNK2 or control shRNA. Control knockdown (left lane) and CNK2 knockdown (right lane) tested by western blot with rabbit anti-CNK2 antibody detecting endogenous CNK2 (upper panel). PSD-95 (middle panel) and Mortalin (lower panel) serve as loading controls (expected size: 60 kDa).

For immunofluorescence experiments, neurons were fixed and stained for the postsynaptic marker Homer1 and the dendritic marker MAP2 **(Fig. 8A)**. As a reflection of PSD size, we quantified the endogenous Homer1 content in spines (DIV21) (Goodman et al., 2017; Meyer et al., 2014). Blinded analysis of the Homer1 immunofluorescence signal area using the "Analyze Particles" tool (FIJI/ImageJ) (Schindelin et al., 2012)

enabled a quantitative comparative analysis of Homer1 immunofluorescence signal intensity and area in neurons expressing either CNK2 shRNA or control shRNA **(Fig. 8B)**. This analysis revealed a clear reduction of PSD size in CNK2 knockdown neurons (overall reduction of 15%; p < 0.0001) **(Fig. 8C)** (Zieger et al., 2019). We also performed a comparative analysis of the spine density in neurons infected with either CNK2 knockdown or control shRNA: here we did not observe substantial differences **(Fig. 8D)**.
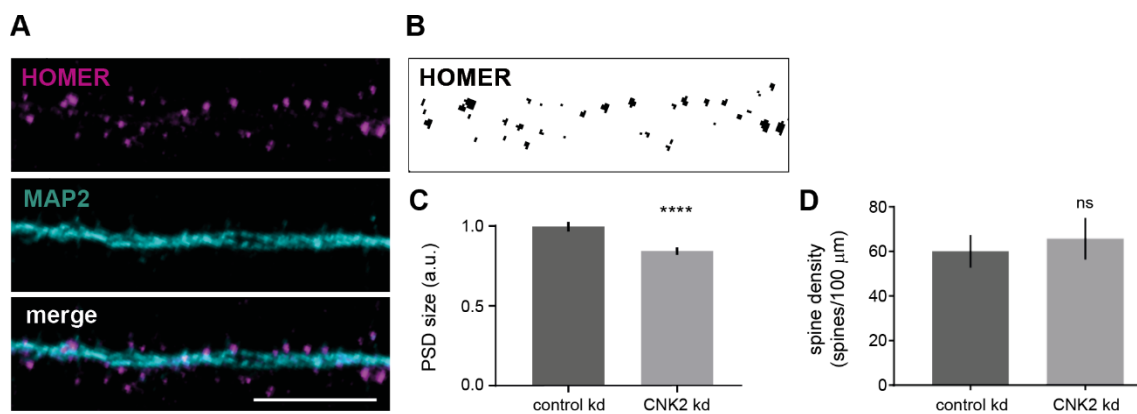
Figure 8: Loss of CNK2 reduces PSD size

(A) Cultured rat hippocampal neuron infected with lentivirus transducing scrambled control shRNA stained with the guinea pig anti-Homer1 antibody for the postsynaptic marker Homer1 (magenta) and the mouse anti-MAP2 antibody for the dendritic marker MAP2 (cyan). Scale bar: 10 µm. (B) Sample image of endogenous Homer1 thresholded for analysis of Homer1 particle size. (C) PSD size, represented by the signal of the postsynaptic marker protein Homer1 (arbitrary units), was analysed using the "Analyze Particles" tool (FIJI/ ImageJ). Data were normalised to the mean of the control. Graph represents the mean ± SEM (n= 757-1100 spines from 7-10 cells, N=3 cultures): control (scrambled shRNA) = 1 ± 0.03, CNK2 knockdown = 0.85 ± 0.02; Mann-Whitney U test, p < 0.0001. (D) Spine density in spines per 100 µm. Graph represents the mean ± SEM (n= 10-13 cells, N=3 cultures): control (scrambled shRNA) = 59.99 ± 7.23, CNK2 knockdown = 65.68 ± 9.27; unpaired t-test, p = 0.6501.

3.3 Expression of the disease-associated CNK2 variant causes increased PSD size and influences synaptic transmission

As mentioned earlier, there are three families reported to carry a mutation leading to an early truncation of the protein. In one case reported (herewith referred to as CNK2-P1), a C>T point mutation causing a change from Arginine into a STOP codon at amino acid 712 (c.2134 C>T; p.Arg712*; NM_014927.5), causes an early truncation of the protein

(Damiano et al., 2017). Another case (in the following named CNK2-P2) refers to a report of three brothers who share a de novo insertion (g.832_3insA, p. D152RfsX8) leading to a frameshift and premature termination (Vaags et al., 2014). A new case report, published very recently (Sun et al., 2018) and for this reason not integrated into experimental aspects of this study, describes a patient carrying a mutation (c.2185 C>T, p.Arg729*; NM_014927.5) that is very similar to CNK2-P1 described above: the premature termination is 17 amino acids further towards the C terminus and the symptoms are very similar to those associated with CNK2-P1. In the experiments described in the next sections, we focussed exclusively on CNK2-P1 and CNK-P2 and took advantage of epitope-tagged expression constructs. For investigation in cultured hippocampal neurons, we expressed these CNK2 variants (see also scheme in **Figure 5A** for overview) fused to an EGFP-tag following lentiviral transduction.

3.3.1 CNK2 mutants

Our aim in studying CNK2 was to understand the molecular consequences of complete loss or mis-function of CNK2 in order to contribute to our understanding of how CNK2 defects cause intellectual disability and seizures. To investigate CNK2 function, we used two approaches. One was to investigate the disease-associated situation, including loss as well as truncation of CNK2 **(Fig. 9A)**. The other one was a more comparative approach: In addition to the reported disease-associated variants, we cloned various deletion constructs **(Fig. 9B)** as tools to explore the function of the different CNK2 domains. These constructs were used in localisation studies and coimmunoprecipitation assays to narrow down the region necessary for certain interactions with CNK2. All constructs depicted in **Figure 9** exhibited solid expression in COS-7 cells. For localisation studies, we overexpressed EGFP-tagged CNK2 mutants in COS-7 cells and explored their subcellular localisation in immunofluorescence experiments **(Fig. 9)**. Those experiments validated that the PH domain is necessary for membrane association, which is in line with earlier studies showing that PH domains bind to phosphatidylinositol lipids in biological membranes (Lemmon, 2008).

Figure 9: Overview of CNK2 constructs and their localisation in COS-7 cells

(A) Scheme and immunofluorescence experiments of CNK2 isoforms and disease associated mutants overexpressed in COS-7 cells. Numbers indicate protein length (amino acids) in the mouse sequence. Domain arcitecture (SAM, sterile alpha motif; CRIC, conserved region in CNK; PDZ, PSD-95/DLG-1/ ZO-1); DUF1170, domain of unknown function; PH, pleckstrin homology). (B) Scheme and immunofluorescence experiments of EGFP-tagged CNK2 mutants overexpressed in COS-7 cells to validate expression and localisation of the mutants. DAPI staining (blue) indicates the nucleus. Scale bar: 10 μm.

3.3.2 PSD size is increased upon expression of disease-associated CNK2

As we already saw an effect of loss of CNK2 on PSD size, we wondered if expression of the disease-associated CNK2-P1 influences PSD size as well. In immunofluorescence experiments we observed an increase in PSD size in neurons expressing EGFP-CNK2-P1 compared to neurons expressing EGFP-CNK2 **(Fig. 10A)**. To make sure that expression of the wild-type and the truncated CNK2 variants were comparable, we analysed whole cell lysates from neurons overexpressing the CNK2 variants by western blot and observed essentially equal expression levels **(Fig. 10C)**. For analysis, images were randomised and analysed blind. As a readout for the (PSD) size we used the postsynaptic marker protein Homer1, as already done in the knockdown experiments described earlier. Defined ROIs along secondary dendrites were analysed using the "Analyze Particles" tool for FIJI, measuring the area represented by the Homer1 signal. In neurons expressing the truncated CNK2 variant (EGFP-CNK2-P1), a fraction of dendritic spines was increased in size significantly **(Fig. 10B)**.

A
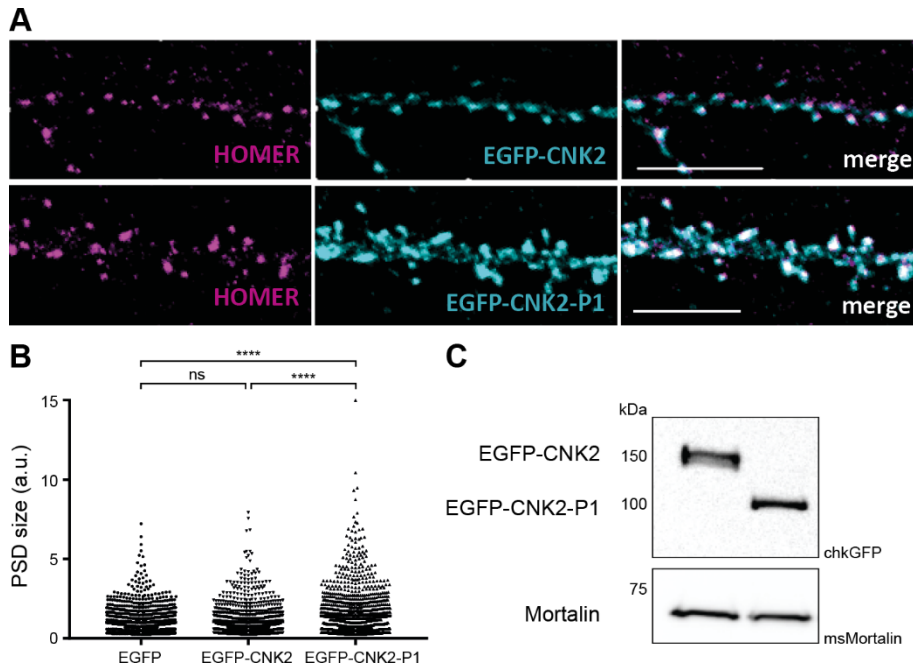
Figure 10: Expression of CNK2-P1 causes increased PSD size

(A) Neurons expressing EGFP-CNK2 or EGFP-CNK2-P1 stained for EGFP (cyan) and Homer1 (magenta). Scale bar: 10 μm (B) PSD size upon expression of EGFP, EGFP-CNK2 or EGFP-CNK2-P1. PSD size, represented by the signal of the postsynaptic marker protein Homer1 (a.u.), was analysed using the "Analyze Particles" tool (FIJI/ImageJ). Data were normalised to the mean of the control (EGFP). Graph represents the mean ± SEM (n= 1184-1366 spines in 13-16 neurons, N=3 cultures); EGFP = 1 ± 0.02, EGFP-CNK2 = 1.05 ± 0.03 or EGFP-CNK2-P1 = 1.43 ± 0.04; data were analysed by Kruskal-Wallis test, followed by Dunn´s multiple comparison test: EGFP vs. EGFP-CNK2: p > 0.9999, EGFP vs. EGFP-CNK2-P1: p < 0.0001; EGFP-CNK2 vs. EGFP-CNK2-P1: p < 0.0001. (C) Western blot of whole cell lysates from cultured hippocampal neurons infected with EGFP, EGFP-CNK2 or EGFP-CNK2-P1; proteins detected by western blot with anti-GFP antibody. Mortalin is used as a loading control.

3.3.3 mEPSC amplitude is increased in neurons expressing disease-associated CNK2

As patients carrying the mentioned CNK2 point mutation have a severe epileptic encephalopathy (Damiano et al., 2017) and the spine size was increased in neurons expressing EGFP-CNK2-P1, we wondered if synaptic transmission is altered by the presence of this truncated CNK2 variant. To address this question, we collaborated with Alexander Stumpf and Dietmar Schmitz (NWFZ, Charité - Universitätsmedizin Berlin). In patch-clamp experiments we investigated synaptic transmission in cultured hippocampal neurons (DIV22-23) infected with EGFP-CNK2 or EGFP-CNK2-P1 at DIV10. During recording, the cells were treated with 1μM Tetrodotoxin (TTX), which selectively blocks voltage-gated sodium channels and this way inhibits the firing of action potential. This enabled us to record spontaneous events, or so-called mini excitatory postsynaptic currents (mEPSCs). We observed a significant increase in the amplitude of

mEPSCs in neurons expressing EGFP-CNK2-P1 compared to neurons expressing EGFP-CNK2 **(Fig. 11A, B)**. However, the frequency of mEPSCs was not altered in those neurons **(Fig. 11A, C)**.
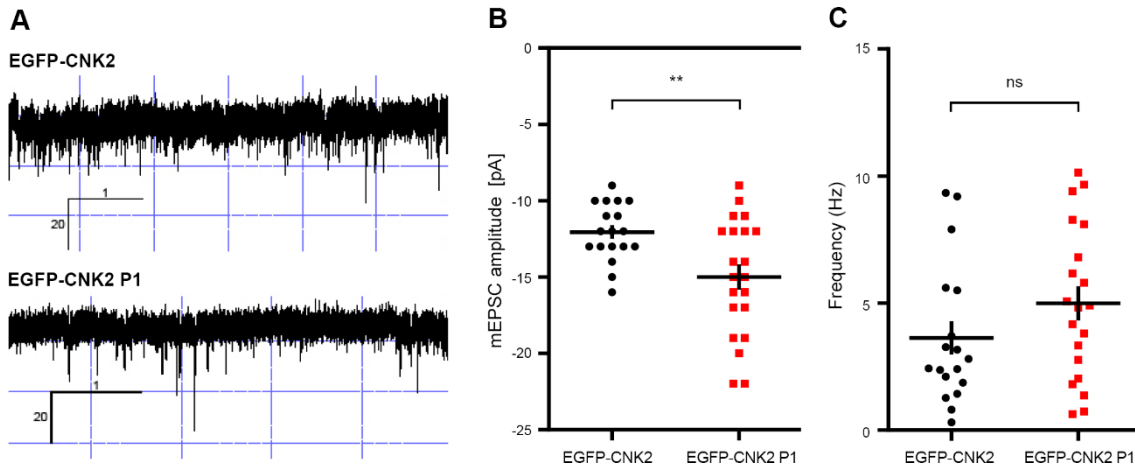
Figure 11: mEPSC amplitude is increased in neurons expressing EGFP-CNK2-P1

(A) Example traces of neurons expressing EGFP-CNK2 (left) or EGFP-CNK2-P1 (right). For recording neurons were treated with 1μM TTX. Recording was included when R_s<20 Ω and I_{hold}<60 pA. (B) mEPSC amplitude was significantly increased in neurons expressing EGFP-CNK2-P1 (red) compared to EGFP-CNK2 (black). (C) Frequency was not altered significantly. Patch clamp experiments and analysis was performed by Alexander Stumpf, NWFZ, Charité Universitätsmedizin-Berlin

3.3.4 Mobility of the disease-associated CNK2 mutant is altered compared to the wild type

As a scaffold protein, CNK2 is an integral component of the PSD, and thereby a participant in the organisation of the synaptic machinery (Li et al., 2017). To date, there are no data about the mobility or exchange rate of CNK2 in dendritic spines. To investigate CNK2 mobility we took advantage of a live-cell imaging technique called fluorescence recovery after photobleaching (FRAP): Fluorescent (most commonly EGFP-tagged) proteins are bleached by a powerful laser pulse in a defined region of interest (ROI), which causes an irreversible loss of fluorescence in a defined area. Subsequently the recovery of fluorescence in the bleached area is measured over time, using a spinning disc microscope. If the bleached protein is diffusing freely, it will be substituted by fluorescent molecules diffusing back into the ROI. Thus, this technique allows us to draw

conclusions about exchange rate and mobility of bleached (non-fluorescent) protein and not bleached (still fluorescent) protein. To address this question, we expressed EGFP-CNK2 and the disease-associated EGFP-CNK2-P1 in cultured hippocampal neurons and measured fluorescence recovery after photobleaching (FRAP) in manually selected dendritic spines **(Fig. 12A)**. Within ten minutes, almost 100% of EGFP-CNK2 was substituted: The mobile fraction of wild-type CNK2 was approximately 95% in the time measured. For the disease-associated variant EGFP-CNK2-P1, total fluorescence recovery was reduced by 22%, indicating that this fraction was essentially immobile (and not exchanged within the recorded time). Half maximal recovery time (t-half) was almost the same for EGFP-CNK2-P1 (0.36 s) compared to EGFP-CNK2 (0.39 s). **(Fig. 12B),** suggesting that exchange dynamics are not affected.
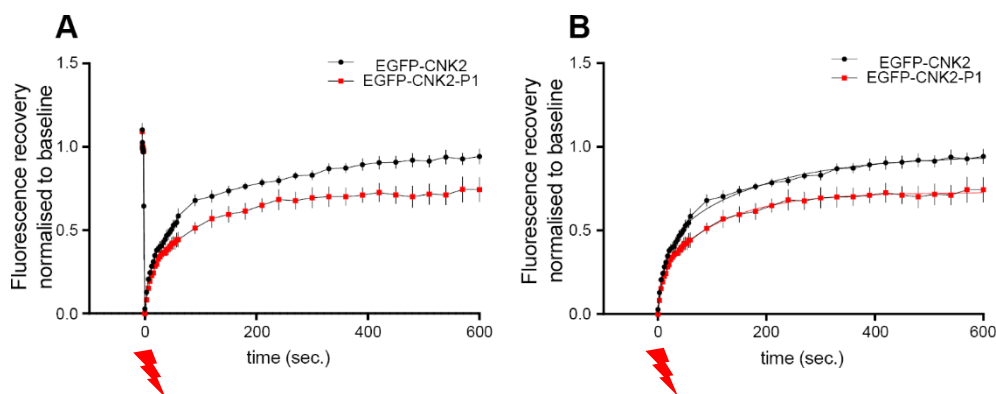
Figure 12: Mobility of CNK2-P1 is reduced compared to the wildtype

(A) FRAP experiment in cultured hippocampal neurons expressing EGFP-CNK2 or EGFP-CNK2-P1. 8-10 spines per neuron were selected manually and defined as ROIs. Photobleaching with a 488 nm laserpulse is indicated at 0 seconds. Fluorescence recovery was measured via live cell image acquisition. Fluorescence intensity was normalised to the mean fluorescence of ten images aquired prior to the bleach. After photobleaching, intensity was recorded for 600 seconds. (B) Graph represents mean ± SEM (n= 9-12 neurons; N= 3 cultures). Plateau: EGFP-CNK2= 0.95 ± 0.04, EGFP-CNK2-P1 = 0.73 ± 0.07; Nonlinear fit. Half maximal recovery time: EGFP-CNK2= 0.39 s, EGFP-CNK2-P1 = 0.36 s.

3.4 Expression of a CNK2 variant that does not bind to the membrane affects PSD size

We observed that loss of CNK2 and accumulation of the disease-associated variant CNK2-P1 influence PSD size in different ways **(Fig. 8C, Fig. 10B)**. We also validated that wild-type CNK2 is membrane-associated in heterologous cells **(Fig. 9A)**. In order to explore the functional importance of its membrane localisation, we used an EGFP-tagged CNK2 deletion construct that lacks the C-terminal region including the PH domain (CNK2ΔPH; see **Fig. 9B**). Following ectopic expression of this mutant, we observed a loss of membrane association **(Fig. 9B)**, which is in line with biochemical studies indicating that PH domains typically bind to phosphatidylinositol lipids in biological membranes (Lemmon, 2008). We expressed this construct in primary hippocampal neurons and compared its expression with EGFP-tagged wild-type CNK2 regarding its influence on spine size. As done for our CNK2 knockdown neurons (see chapter 3.2) and exploration of CNK2-P1 in neurons (see chapter 3.3.2), we utilised a quantitative comparative immunofluorescence approach to analyse protein content in dendrites and spines. We first assessed the general expression of wild-type EGFP-CNK2 and EGFP-CNK2ΔPH in dendrites by comparing EGFP signal intensity relative to the dendritic marker MAP2 (see

Fig. 13A), and we observed that CNK2ΔPH expression is reduced in secondary dendrites compared to the wild-type CNK2 (Zieger et al., 2019). Using this method, we conclude that the amount of EGFP-CNK2ΔPH in dendrites is reduced by almost 65% compared to the wild-type **(Fig. 13B)** (Zieger et al., 2019). To make sure that this was not an effect of globally reduced expression of the truncated CNK2 variant, we analysed whole cell lysates from neurons expressing the CNK2 variants by western blot and observed comparable expression levels **(Fig. 13C)** (Zieger et al., 2019). These observations suggest that this difference did not simply reflect reduced total expression of EGFP-CNK2ΔPH but rather reflected an altered localisation.
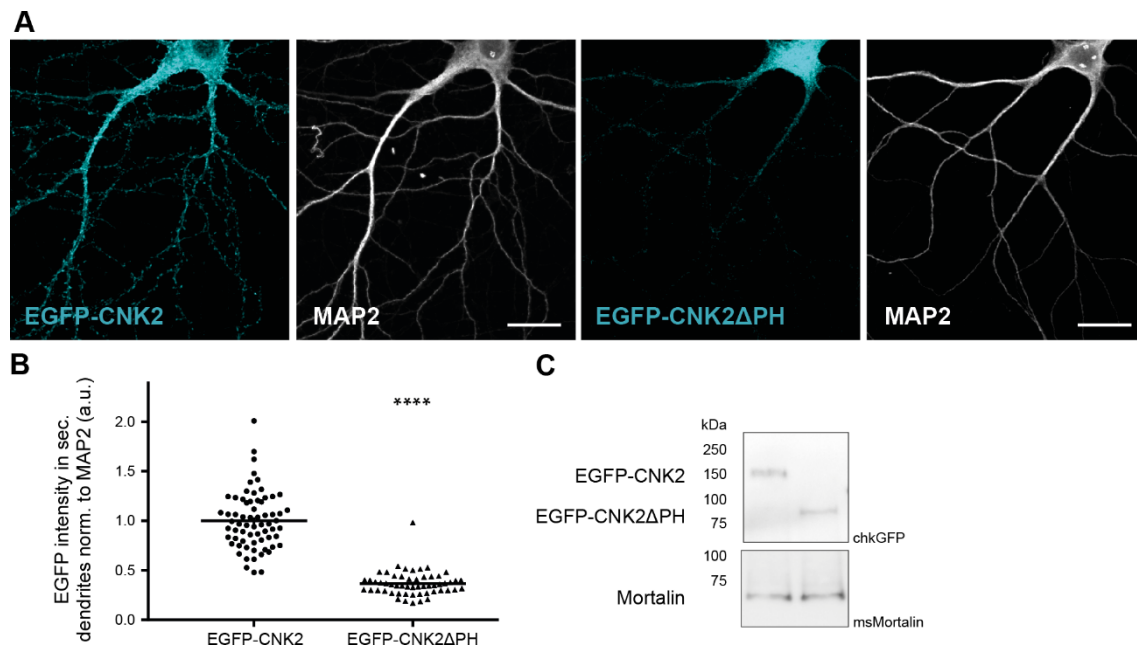
Figure 13: The CNK2 variant that does not bind to the membrane is mis-localised in neurons

(A) Representative images of primary neurons expressing either EGFP-CNK2 (cyan) or EGFP-CNK2ΔPH (cyan) co-stained with guinea pig anti-MAP2 antibody for endogenous MAP2 (grey). Scale bar: 20 μm. (B) Quantification of amount of EGFP-CNK2 and EGFP-CNK2ΔPH based on EGFP- signal intensity (a.u.) normalised to MAP2 signal intensity in regions of interest (ROIs) along secondary dendrites. Data were normalised to the mean of the control. Graph represents mean ± SEM (arbitrary units, a.u.) of EGFP intensity (n= 55-67 ROIs in 11-14 neurons, N=3 cultures): EGFP-CNK2 = 1 ± 0.04, EGFP-CNK2ΔPH = 0.37 ± 0.02, data were analysed by Mann-Whitney U test, p < 0.0001. (C) Western blot of whole cell lysates from cultured hippocampal neurons infected with EGFP-CNK2 or EGFP-CNK2ΔPH; proteins detected by western blot with chicken anti-GFP antibody. Mortalin is used as a loading control.

Next, we comparatively assessed the expression of the postsynaptic protein Homer1 **(Fig. 14A)**. Again, following blinded analysis of Homer1 in spines, we observed a reduction of

Homer1 content in the dendritic spines **(Fig. 14B)** (Zieger et al., 2019) as well as a trend towards reduced spine density of neurons expressing EGFP-CNK2ΔPH when compared to neurons expressing the wild-type EGFP-CNK2 or EGFP alone **(Fig. 14C).** In summary, we conclude that, compared to neurons expressing EGFP-CNK2, neurons expressing the non-membrane-associated EGFP-CNK2ΔPH have reduced Homer1 content in spines. This result indicates that mis-localised CNK2 can also interfere with regulation of PSD size. Interestingly we see the same upon loss of CNK2 (see **Fig. 8**).
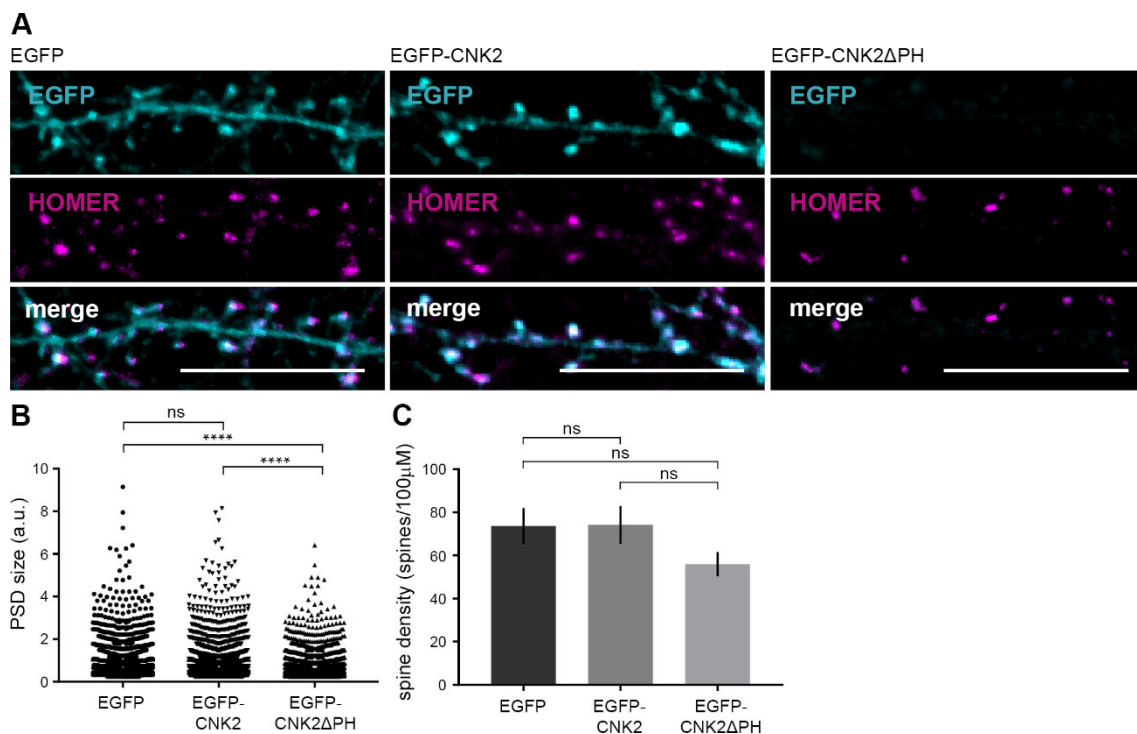
Figure 14: Expression of a CNK2 variant that does not bind to the membrane affects spine morphology

(A) Neurons expressing EGFP, EGFP-CNK2 or EGFP-CNK2ΔPH stained for EGFP (cyan) and Homer1 (magenta). Scale bar: 10 μm. (B) Postsynaptic density (PSD) size upon expression of EGFP, EGFP-CNK2 or EGFP-CNK2ΔPH. PSD size, represented by the signal of the postsynaptic marker protein Homer1 (a.u.), was analysed using the "Analyze Particles" tool (FIJI/ImageJ). Data were normalised to the mean of the control. Graph represents the mean ± SEM (n= 1555-2008 spines in 14-18 neurons, N=4 cultures); EGFP = 1 ± 0.02, EGFP-CNK2 = 0.99 ± 0.02, EGFP-CNK2ΔPH = 0.81 ± 0.02; data were analysed by Kruskal-Wallis test, followed by Dunn´s multiple comparison test: EGFP vs. EGFP-CNK2: p = 0.343, EGFP vs. EGFP-CNK2ΔPH: p < 0.0001; EGFP-CNK2 vs. EGFP-CNK2ΔPH: p < 0.0001. (C) Spine density upon expression of EGFP, EGFP-CNK2 or EGFP-CNK2ΔPH was analysed counting spines positive for Homer1. Graph represents number of spines per 100 μm dendrite. Data are representative for the mean ± SD (a.u.) n= 11-14 neurons per condition, N= 3 cultures: EGFP = 73.67, EGFP-CNK2 = 74.18 or EGFP-CNK2ΔPH = 55.94, ordinary one-way ANOVA, followed by Tukey´s multiple comparison test: EGFP vs. EGFP-CNK2: p = 0.9988, EGFP vs. EGFP-CNK2ΔPH: p = 0.2698, EGFP-CNK2 vs. EGFP-CNK2ΔPH: p= 0.2110

3.5 The kinases MINK and TNIK are novel interaction partners of CNK2

3.5.1 Y2H screen to identify novel interaction partners

To further investigate the role of CNK2 in neurons, we next focussed on novel CNK2 interaction partners, which we identified via a yeast-two-hybrid screen of cDNAs from adult mouse brain together with Hybrigenics. The bait, full-length CNK2 (mus musculus, Gene ID: 245684, aa 1-1032), cloned into pB27 (N-LexA-bait-C fusion) was used to screen an adult mouse brain cDNA library.

The list of interactors we obtained from the Y2H screen included proteins with diverse functions, and a significant fraction of positive hits were signalling proteins, *e. g.* ARHGAP39, Cytohesin1 and Cytohesin4, MAGI3 and the kinases MINK1 and TNIK **(Table 14)**. The success of our Y2H screen was validated, as our list included the Rho-GTPase activating protein Vilse/ARHGAP39, and the guanine-nucleotide exchange activating proteins Cytohesin1 and Cytohesin4, which had previously been shown to interact with CNK2 using other methods (Lim et al., 2014). Two proteins identified in our screen, the kinases TNIK and MINK1, were of special interest to us, in part because they have both been implicated in the regulation of neuron structure and glutamate receptor function (Hussain et al., 2010). In addition, TNIK was recently shown to be associated with intellectual disability in patients (Anazi et al., 2016), and TNIK knockout mice exhibit cognitive impairment and hyperactivity (Coba et al., 2012). Moreover, this protein was recently investigated for its role in the regulation of protein complexes in PSDs (Li et al., 2017).

Table 14: Yeast-two-hybrid screen of cDNAs form adult mouse brain

List of interaction partners of full-length CNK2 (mus musculus, Gene ID: 245684, aa 1-1032), identified in the yeast-two-hybrid screen performed together with Hybrigenics.

Gene Name	Function	Gene ID	Interaction domain (aa)	Clones detected
Arhgap39	Rho GTPase activating protein 39	223666	1-319	2
Cytohesin1	Mediates the regulation of protein sorting and membrane trafficking, Promotes guanine-nucleotide exchange on ARF1 and ARF5. Promotes the activation of ARF through replacement of GDP with GTP.	19157	14-100	7
Cytohesin4	Promotes guanine-nucleotide exchange on ARF1 and ARF5. Promotes the activation of ARF through replacement of GDP with GTP	72318	6-235	5
Magi3	Membrane-associated guanylate kinase	99470	63-656	1
Mink1	Ste 20 kinase. Regulator of neuronal structure and AMPA receptor trafficking, as well as surface AMPA receptor expression. Required for normal synaptic density, dendrite complexity. Regulates MAPK pathways and mediates stimulation of the stress-activated protein kinase p38 MAPK downstream of the Raf/ERK pathway. Involved in the regulation of actin cytoskeleton reorganization, cell-matrix adhesion, cell-cell adhesion and cell migration.	50932	430-533	4
Samd12	Disease associated, SAM domain containing protein 12	320679	41-161	3
Sox5	Transcriptionfactor	20678	351-582	1
Tnik	Ste 20 kinase, disease-associated (ID) Regulates activity and degradation of PSD proteins. Required for dendritic arborisation, branching and spine density. Influences AMPAR trafficking and synaptic transmission. Plays a role in actin regulation, organisation of the cytoskeleton and cell morphology. Regulates postsynaptic and nuclear signalling pathways.	665113	337-598	1

3.5.2 CNK2 interacts with MINK1 and TNIK and regulates their localisation

MINK1 and TNIK have common domain architecture, with a kinase domain at the N-terminus and a Citron Homology Domain (CNH) at the C-terminus, but exhibit minimal sequence homology outside of their conserved domains **(Fig. 15A)**. We demonstrated that CNK2 interacts with both TNIK and MINK1 in co-immunoprecipitation assays **(Fig. 15B, C)**. Interestingly, the ubiquitously expressed CNK1 protein, which shares several interaction domains with CNK2 **(Fig. 15A)**, did not interact with TNIK or MINK1 in comparable assays **(Fig 15B, C)**, suggesting that the CNK2-TNIK and CNK2-MINK1 interactions may have CNK2-specific functions that are important in neurons (Zieger et al., 2019).
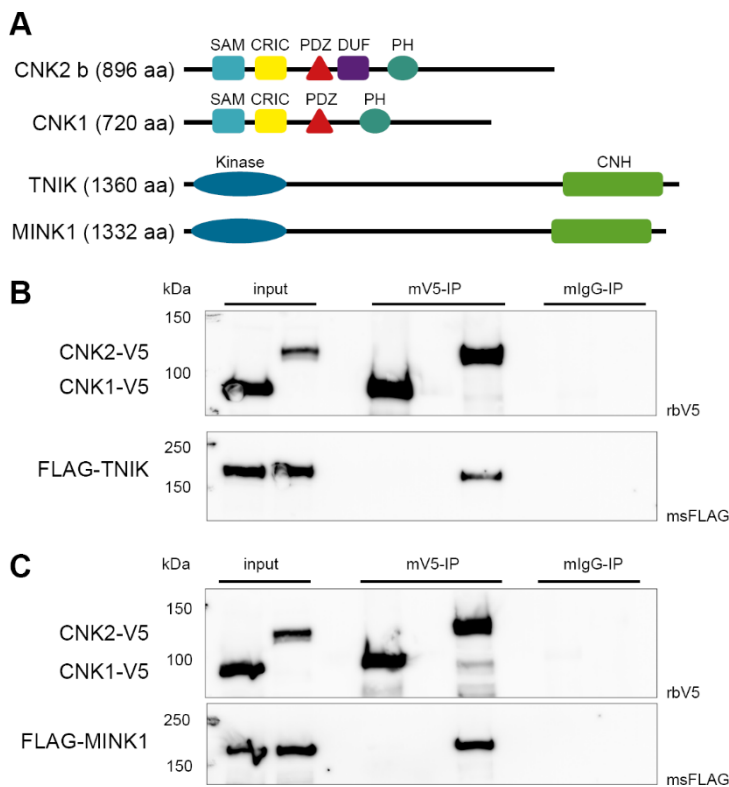
Figure 15: CNK2 interacts with TNIK and MINK1

(A) Scheme of CNK1 and CNK2 domain architecture: (SAM, sterile alpha motif; CRIC, conserved region in CNK; PDZ, PSD-95/DLG-1/ZO-1; DUF1170, domain of unknown function; PH, pleckstrin homology); Scheme of MINK1 and TNIK domain architecture: (Kinase domain, CNH, Citron Homology Domain). (B) CNK2 specifically interacts with TNIK. Coimmunoprecipitation experiment with CNK1-V5, CNK2-V5 and FLAG-TNIK expressed in COS-7 cells. Proteins were immunoprecipitated with either anti-V5 (mouse) antibody or mouse IgGs as a negative control. Proteins were detected by western blot with rabbit anti-V5 (CNK2) and mouse anti-FLAG (TNIK) antibodies. (C) CNK2 specifically interacts with MINK1. Coimmunoprecipitation experiment with CNK1-V5, CNK2-V5 and FLAG-MINK1 overexpressed in COS-7 cells. Proteins were immunoprecipitated with either anti-V5 (mouse) antibody or normal mouse IgG as anegative control. Proteins were detected by western blot with rabbit anti-V5 (CNK2) and mouse anti-FLAG (MINK1) antibodies.

3.5.3 TNIK and MINK1 localisation is regulated by CNK2

In a subsequent set of experiments, we narrowed down the region within CNK2 that is relevant for TNIK or MINK1 binding. Using a set of EGFP-tagged CNK2 deletion constructs with C-terminal truncations of various lengths **(Fig. 16A)**, we demonstrated via co-immunoprecipitation that loss of the C-terminal region harbouring the PH domain had no effect on TNIK or MINK1 binding. Deletion of both PH and DUF domains, however, did affect binding affinity. Most notably, when the PDZ domain was deleted together with the PH and DUF domains, binding to TNIK **(Fig. 16B)** and MINK1 **(Fig. 16E)** was completely abolished. Together, these results indicate that the region including the PDZ and the DUF domain is critical for CNK2 binding to TNIK and MINK1, and that a CNK2 variant lacking only the PH domain / C-terminus responsible for membrane localisation is still capable of efficient binding to these new interacting proteins (Zieger et al., 2019).

We next took advantage of this MINK/TNIK-binding deletion construct (EGFP-CNK2ΔPH) to explore the idea that CNK2 might functionally influence TNIK or MINK1. We observed earlier that full-length CNK2 exhibits a clear membrane localisation in heterologous cells **(Fig. 5, 9A)**. Immunofluorescence of ectopically expressed FLAG-TNIK or FLAG-MINK1 together with EGFP as a control in COS-7 cells indicated that neither TNIK **(Fig. 16C, upper panel)** nor MINK1 (data not shown) is enriched at the membrane. However, upon co-expression with full-length CNK2, TNIK **(Fig. 16C, middle panel)** as well as MINK1 **(Fig. 16F, upper panel)** was observed at the membrane in most cells, suggesting that CNK2 might play an important role in regulating the subcellular localisation of both kinases. In order to confirm the specificity of this observation, we took advantage of the CNK2ΔPH mutant described earlier. Upon co-transfection of EGFP-CNK2ΔPH, TNIK was no longer at the membrane **(Fig. 16C, lower panel)**, suggesting that binding to wild-type CNK2 is indeed a mechanism that facilitates TNIK membrane localisation. A comparable experiment with CNK2 and MINK1 indicates that the same is true for this protein-protein interaction **(Fig. 16F)**, *i.e.* our data

suggest that CNK2 is capable of influencing the membrane localisation of both kinases (Zieger et al., 2019).

We next quantified these results following blinded analysis of TNIK membrane localisation in cells co-transfected with TNIK and either wild-type or mutant CNK2 proteins **(Fig. 16D)**. This quantification clearly demonstrates that localisation of TNIK is influenced by CNK2 localisation in heterologous cells (Zieger et al., 2019).
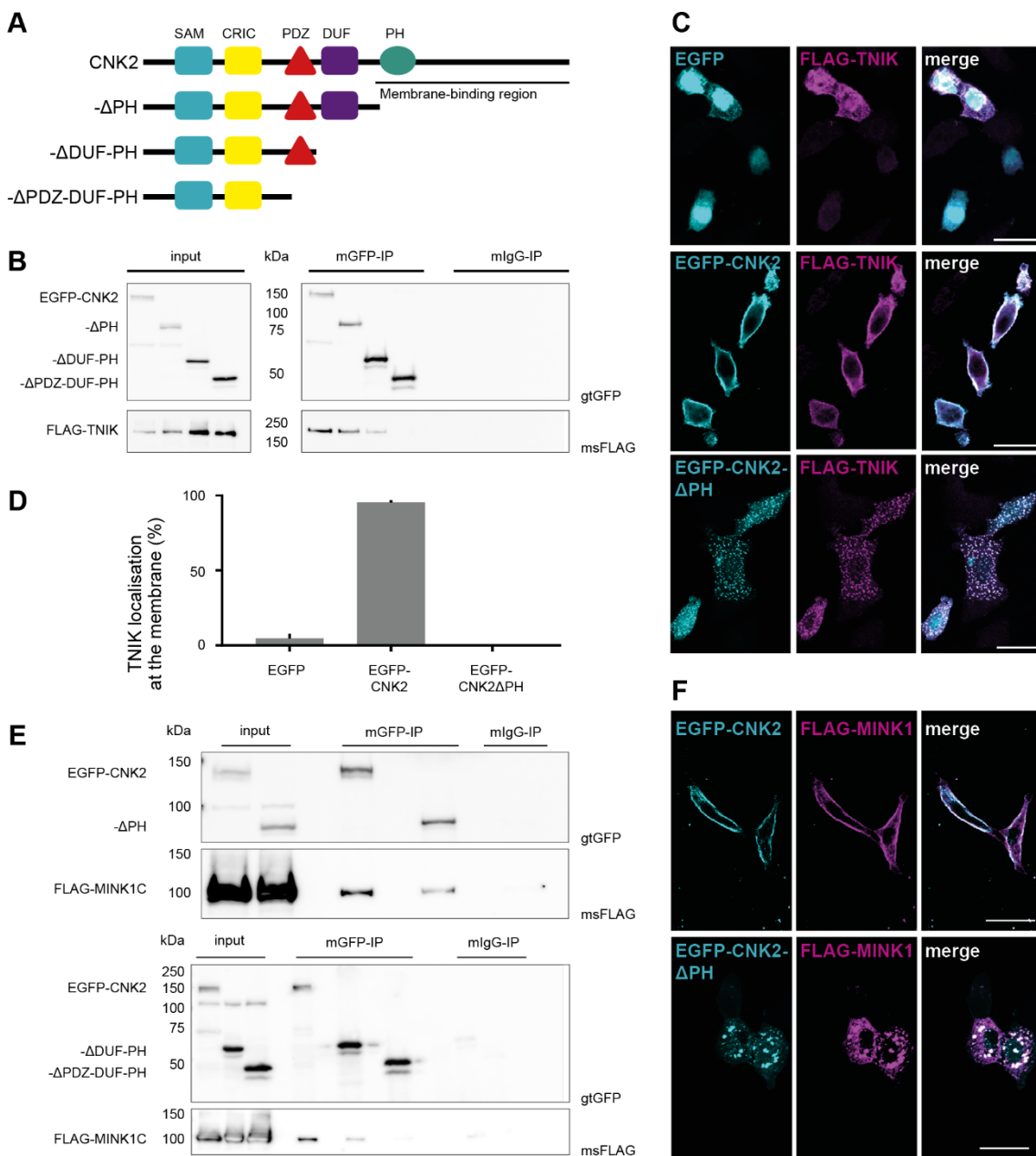
Figure 16: The DUF- and the PDZ domain of CNK2 are important for interaction with MINK1 and TNIK and localisation of MINK1 and TNIK is regulated by CNK2

(A) Scheme of CNK2 truncation variants (for detailed description of domains see Fig. 9A legend). (B) Co-immunoprecipitation experiments of EGFP-CNK2 variants overexpressed in COS-7 cells together with FLAG-TNIK. Proteins were immunoprecipitated with either anti-GFP (mouse) antibody or mouse IgGs as a negative control. Pull-down control and coprecipitated proteins were analysed by western blot with anti-GFP (IP) and anti-FLAG (coIP) antibodies. Input control (lysate) is shown on the left. (C) TNIK localisation is influenced by CNK2 in heterologous cells. Representative immunofluorescence experiments in COS-7 cells overexpressing FLAG-TNIK together with EGFP as control (upper panel), EGFP-CNK2 (middle panel) or EGFP-CNK2ΔPH (lower panel). Left panels show EGFP only or EGFP-tagged CNK2 variants (cyan), middle panels shows FLAG-TNIK (magenta), and the right lane shows merged channels. Scale bar: 20 μm. (D) For quantification of TNIK localisation in COS-7 cells reflecting the experiments shown in (C), images expressing both proteins, were randomised and classified according to cytosolic or membranous TNIK localisation. Co-expression of CNK2 recruits the main fraction of FLAG-TNIK to the membrane. Upon co-expression of EGFP-tagged CNK2 variants lacking the membrane binding region, FLAG-TNIK shows essentially no membranous localisation. Data used for quantification include data for a total of 73-114 cells per condition, imaged from three independent experiments. (E) Coimmunoprecipitation experiments of EGFP-CNK2 variants overexpressed in COS-7 cells together with FLAG-MINK1C (aa 534-1301). Proteins were immunoprecipitated with either anti-GFP (mouse) antibody or normal mouse IgG as negative control. Proteins were detected by WB with with anti-GFP (IP) and anti-FLAG (coIP) antibodies . Input control (lysate) is on the left. (F) Immunofluorescence experiment in COS-7 cells expressing FLAG-MINK1 together with EGFP-CNK2 (upper panel) or EGFP-CNK2ΔPH (lower panel); Left lane shows EGFP-tagged CNK2 variants (cyan), middle lane shows FLAG-MINK1 (magenta), and right lane shows merged channels. Scale bar: 20 μm.

3.5.4 Mis-localisation of CNK2 influences TNIK localisation in neurons

Subsequent cell-based studies focussed on the CNK2-TNIK interaction. We first investigated whether CNK2 and TNIK indeed reside in the same subcellular compartments. Using antibodies to the endogenous proteins, we could show by immunofluorescence on cultured primary rat hippocampal neurons (DIV21) that CNK2 and TNIK co-localise in dendritic spines **(Fig. 17A)**, providing further support for the idea that these two proteins can indeed function together at postsynaptic sites. We also confirmed that endogenous TNIK binds CNK2 in neural tissue: following immunoprecipitation of EGFP-CNK2 expressed in primary rat hippocampal neurons at DIV21, we could detect coprecipitated TNIK by western blot analysis **(Fig. 17B)** (Zieger et al., 2019).
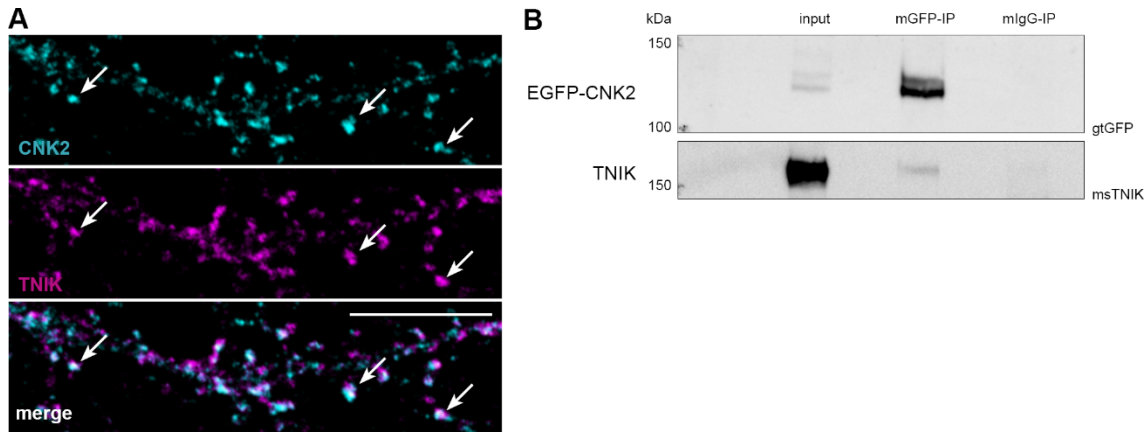
Figure 17: Endogenous TNIK colocalises and interacts with CNK2 in neurons

(A) Representative image of a primary neuron (DIV 21) stained with guinea pig anti CNK2 for endogenous CNK2 (cyan) and with mouse anti TNIK antibody for endogenous TNIK (magenta) in dendritic spines. Scale bar: 10 μm (B) Coimmunoprecipitation experiment of EGFP-CNK2 with endogenous TNIK expressed in neurons. Proteins were immunoprecipitated with either anti-GFP (mouse) or mouse IgGs as a negative control and detected by western blot with anti-GFP (CNK2) and anti-TNIK antibodies. Input control (lysate) is shown on the left.

To gain further insight into the CNK2-mediated regulation of TNIK in neurons, we examined the precise neuronal localisation of TNIK in neurons expressing either wild-type EGFP-CNK2 or EGFP-CNK2ΔPH. Immunofluorescence of EGFP-tagged proteins in neurons confirmed that – as in heterologous cells – EGFP-CNK2ΔPH exhibited an aberrant localisation in neurons: compared to wild-type CNK2, this truncated version was expressed at reduced levels in dendrites; instead, it seemed to be localised mainly in the soma and in the nucleus, which was not the case for full-length EGFP-CNK2 **(Fig. 13A, B; 18A left panel, B left panel)**. As we showed earlier **(Fig. 6)**, full-length CNK2 is observed primarily in dendrites and in spines. We next assessed TNIK localisation in neurons expressing either full-length or truncated CNK2 variants. Cultured rat hippocampal neurons expressing either EGFP alone, EGFP-CNK2 or EGFP-CNK2ΔPH were analysed with regard to TNIK content and localisation **(Fig. 18B)**. We normalised endogenous TNIK signal to the signal for the dendritic marker MAP2 and used a quantitative immunofluorescence approach that involved a blinded selection and analysis of the images. On average, the intensity of endogenous TNIK in secondary dendrites was reduced significantly by up to 18% in neurons expressing EGFP-CNK2ΔPH

51

compared to neurons expressing EGFP-CNK2 or EGFP alone (**Fig. 18C**, for overview see **Fig. 18A left panel**). These data suggest that mis-localisation of EGFP-CNK2ΔPH, which binds to TNIK, indeed seems to trap TNIK in the soma, thereby resulting in reduced total TNIK in the dendrites (Zieger et al., 2019). It has been shown that endogenous TNIK is naturally localised in the postsynapse of wild-type neurons (Burette et al., 2015). We explored the idea that loss of CNK2 might also influence TNIK localisation, but we could not observe a significant difference of TNIK content in dendrites following virus-mediated shRNA knockdown of CNK2 in neurons (data not shown). However, the amount of endogenous TNIK in the dendrites is clearly reduced in neurons expressing the mis-localised truncated CNK2 (EGFP-CNK2ΔPH, **Fig. 18B**, for overview see **Fig. 18A middle panel**). This result is in line with our data from heterologous cells, and suggests that this mutant is capable of interfering with normal CNK2-mediated regulation of TNIK localisation in neurons.
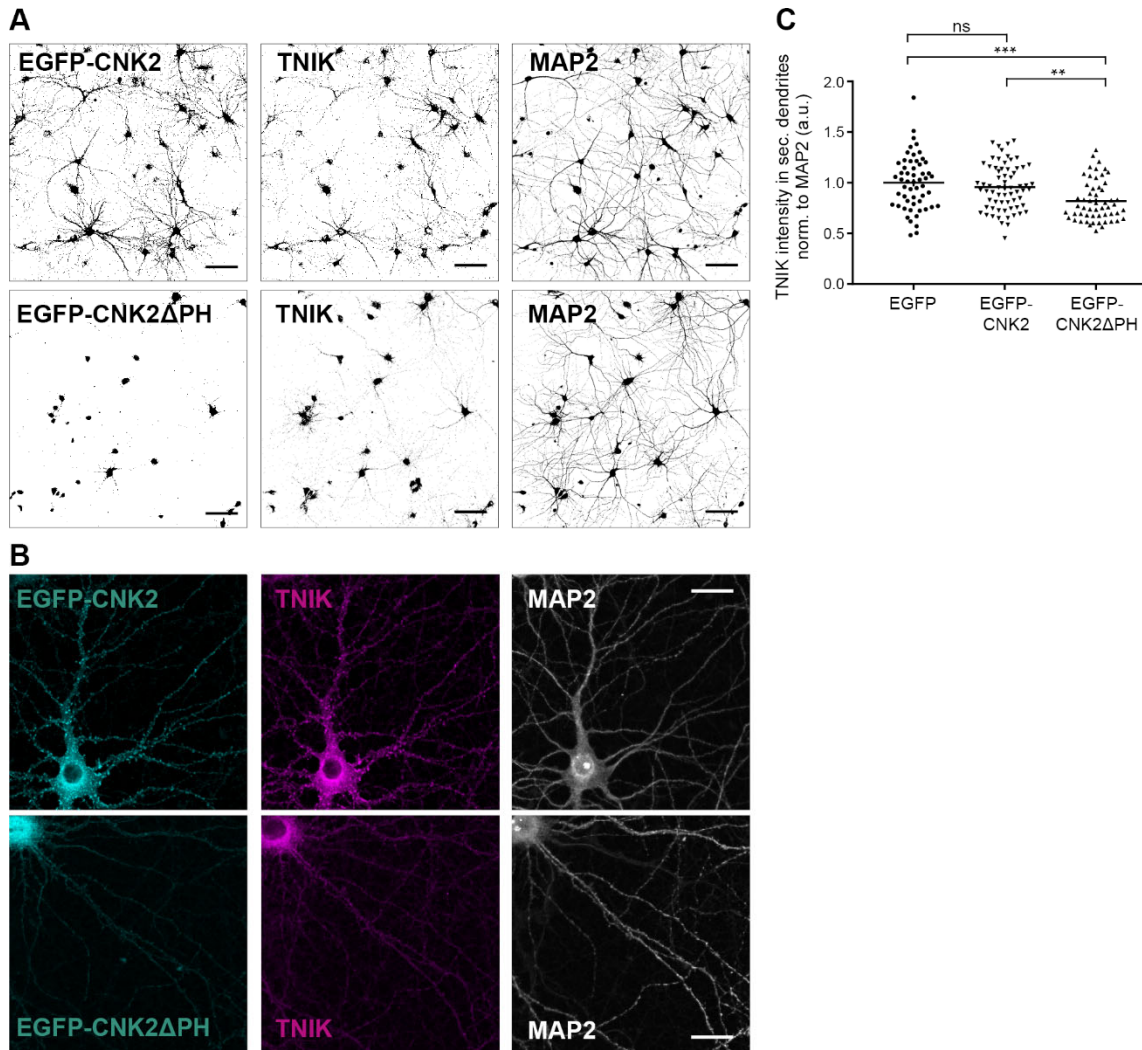
Figure 18: Mis-localisation of CNK2 also influences TNIK localisation in neurons

(A) Overview images of neurons converted to binary images (DIV23) expressing EGFP-CNK2 or EGFP-CNK2ΔPH following viral-mediated gene delivery (left panel). Neurons are stained for endogenous TNIK (middle panel) and endogenous MAP2 (right panel), indicating the general dendritic structure of neurons. Thresholds are set identical for each panel (EGFP/TNIK/MAP2). Scale bar: 100 µm. (B) Images of cultured rat hippocampal neurons expressing EGFP-CNK2 (cyan) or EGFP-CNK2ΔPH (cyan) following viral-mediated gene delivery co-stained for endogenous TNIK (magenta) and MAP2 (grey). Scale bar: 20 µm (C) Co-expression of EGFP-CNK2ΔPH causes a reduction of TNIK in secondary dendrites compared to EGFP or EGFP-CNK2. TNIK fluorescence intensity was measured in ROIs along secondary dendrites and normalised to MAP2 intensity (a.u.). Data were normalised to the mean of TNIK intesity in neurons expressing EGFP only. Graph represents mean ± SEM of TNIK intensity in ROIs of sec. dendrites (n= 55-67 ROIs in 11-14 neurons, N=3 cultures): EGFP = 1 ± 0.04, EGFP-CNK2 = 0.96 ± 0.03 EGFP-CNK2ΔPH = 0.82 ± 0.03, data were analysed by ordinary one-way ANOVA, followed by Dunnett´s post-hoc test: EGFP vs. EGFP-CNK2: p = 0.474; EGFP vs. EGFP-CNK2ΔPH: p = 0.0001; EGFP-CNK2 vs. EGFP-CNK2ΔPH: p = 0.0027

3.6 CNK2 forms a complex with JNK and TNIK

3.6.1 JNK1 and JNK3 are novel interaction partners of CNK2

In a computational high-throughput study the coding sequences of the human genome were screened for a very specific amino acid sequence serving as JNK docking site (Whisenant et al., 2010). Among other proteins, CNK1 and CNK2 came up in this screen, suggesting that these proteins may be JNK substrates and thus are also putative interaction partners. We could confirm an interaction in coimmunoprecipitation assays from COS-7 cells overexpressing CNK2 with JNK1 or JNK3 **(Fig. 19)**. Differing from our results on CNK2-mediated effects on TNIK, in immunofluorescence experiments where we coexpressed CNK2 mutants with JNK3, we could not see an influence of CNK2 on JNK3 localisation in COS-7 cells (data not shown). However, given that others have shown that TNIK regulates JNK phosphorylation (Fu et al., 1999; Larhammar et al., 2017), our observations that CNK2 is physically linked to both JNKs and TNIK suggests that CNK2 may by capable of modulating this functional link between TNIK and JNKs.
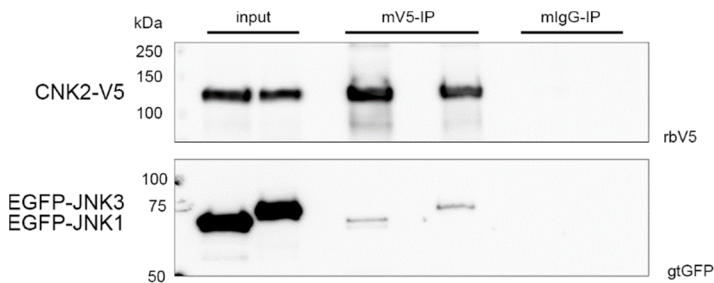
Figure 19: JNK1 and JNK3 are novel interaction partners of CNK2

CNK2 specifically interacts with JNK1 and JNK3. Coimmunoprecipitation experiment with CNK2-V5, EGFP-JNK1 and EGFP-JNK3 expressed in COS-7 cells. Proteins were immunoprecipitated with either mouse anti-V5 antibody or mouse IgGs as a negative control. Proteins were detected by western blot with rabbit anti-V5 (CNK2) and goat anti-GFP (JNK) antibodies.

4. Discussion

4.1 Regulation of PSD size by CNK2 and other disease-associated scaffold proteins

There are many studies about the link between disease-associated postsynaptic scaffold proteins and spine morphology. Within the PSD, an equilibrium of structural and catalytically active proteins is crucial for normal synaptic function and development. There are multiple studies on how disease-associated synaptic proteins affect spine size and/or density. One example is the disease-associated PSD scaffold protein SH3 and multiple Ankyrin repeat domains protein (SHANK). The SHANK family of proteins are a set of scaffold proteins that are present at glutamatergic synapses and represented by three genes: SHANK1, SHANK2 and SHANK3. SHANK proteins have various domains and interact with multiple PSD proteins, including *e. g.* GKAP and Homer (Sheng and Kim, 2011); they also play an important role in receptor trafficking and synaptic signalling (for reviews, see (Monteiro and Feng, 2017)) Mutations in the SHANK genes have been implicated in Phelan-McDermid syndrome (Boccuto et al., 2013; Durand et al., 2007; Watt et al., 1985) and autism spectrum disorders (ASD) (Moessner et al., 2007; Monteiro and Feng, 2017). In ASD patients, various SHANK alterations have been identified. These mutations include insertions, deletions, and point mutations. Experiments in neurons of SHANK knockout mice showed that loss of SHANK causes reduction of PSD thickness and length, reduced PSD protein levels *e.g.* reduced Homer, PSD-93, GKAP, AMPA and NMDA receptor subunits, as well as reduced spine density (Hung et al., 2008; Peca et al., 2011; Wang et al., 2011b). Overexpression of SHANK promoted morphological maturation and formation of mushroom spines in immature neurons (DIV7), and mature neurons (DIV18) overexpressing SHANK showed enlarged spine heads compared to control neurons (Sala et al., 2001). Further, SHANK proteins were shown to be involved in the organisation of AMPAR subunit composition in developing neurons (Ha et al., 2018).

Another highly abundant scaffold protein is Homer. Homer scaffold proteins play a major role in synaptogenesis and plasticity (de Bartolomeis et al., 2014; Guang et al., 2018) and have been associated with schizophrenia and dementia (Iasevoli et al., 2013; Szumlinski et al., 2006). The effect of Homer1a, the activity-inducible short splice variant of Homer1, on spine morphology has been explored in experiments in dissociated cultures of hippocampal neurons (DIV16 - DIV17): Overexpression of Homer1a caused a reduction in spine size and number (Sala et al., 2003). Interestingly, when investigating the effect of Homer1a on other synaptic proteins, reduction in the synaptic cluster size of SHANK as well as PSD-95 and GKAP could be observed (Sala et al., 2003). These data on the disease-associated scaffold proteins SHANK and Homer illustrate that alterations of protein levels can have drastic effects on synapse morphology and function.

When we started to investigate morphological changes in neurons expressing different CNK2 variants, we observed visible differences in spine size upon initial analysis of fluorescent signals using a confocal microscope. After testing several approaches to quantitatively analyse the observed changes in spine size, we chose Homer staining as a readout for the PSD, as it was used as a marker for PSD size in previous studies (Goodman et al., 2017; Meyer et al., 2014). Our selection of Homer for this purpose, instead of the commonly used PSD marker protein PSD-95 is based on the fact that CNK2 interacts with PSD-95 in our hands (data not shown). PSD-95 would not serve as a reliable readout for PSD size, as mislocalisation of CNK2 could directly influence PSD-95 localisation and the results would be biased.

In this study, we observed that CNK2 expression influences PSD size. Measuring the Homer cluster size in CNK2 knockdown neurons and in neurons expressing selected variants of CNK2 led to the conclusion that accumulation of truncated CNK2 in dendritic spines increases PSD size, whereas reduction of CNK2 levels – upon knockdown or mislocalisation – decreases PSD size. From this data, we can conclude that balanced CNK2 expression and regulation are important for normal spine formation and maintenance. The tendency towards reduced spine density that we observe in neurons expressing a CNK2 variant that does not localise to the membrane is something we do

not observe in the CNK2 knockdown condition. One reason for this could be the time point of lentiviral infection: CNK2 knockdown was infected at DIV3, the CNK2 expression constructs at DIV10. *In vitro*, the spine formation of neurons takes place from DIV10 - DIV18 (Nwabuisi-Heath et al., 2012). Our data indicate that expression of a dominant negative CNK2 variant from DIV10 on has a negative effect on spine formation. However, complete loss of CNK2 at earlier stages in development seems to be compensated.

4.2 The role of TNIK in neurons

Kinases are enzymes that phosphorylate their substrates and this way regulate protein function. They are involved in major signalling pathways in neurons and play an important role in synaptic function (Baltussen et al., 2018). Misshapen-like kinase 1 (MINK1 or MAP4K6) and Traf2- and Nck-interacting kinase (TNIK or MAP4K7) are members of the Ste20 family of the MAP4 kinases, *i.e.* they act upstream of MAP kinase cascades. The domain structure of MINK1 and TNIK (see scheme Fig. 15) is characterised by a kinase domain at the N-terminus and a Citron homology (CNH) domain at the C-terminus, which are separated by an intermediate part (Dan et al., 2001). Both kinases are highly expressed in the brain, and they are components of the PSD of glutamatergic synapses (Burette et al., 2015; Hussain et al., 2010). In a recent genetic study, TNIK was implicated in ID (Anazi et al., 2016). TNIK is a regulator of neuronal morphology, as loss of TNIK reduces dendritic arbor complexity as well as spine density (Burette et al., 2015; Hussain et al., 2010; Wang et al., 2011a). Interestingly, it has been proposed by others that TNIK is involved in the regulation of synaptic protein content (Wang et al., 2011a). Previous studies showed that TNIK is a critical signalling molecule regulating degradation of postsynaptic proteins: PSD proteins like the scaffold protein PSD-95, and the transmembrane AMPA receptor regulatory protein TARPγ2 (also commonly referred to as Stargazin) are stabilised by TNIK, and inhibition of TNIK activity leads to reduction in PSD protein levels (Wang et al., 2011a). Further, Wang et al. report a decrease in size and density of PSD-95 and surface GluR1 clusters upon inhibition of TNIK (Wang et al.,

2011a). This is supported by a proteomics study from 2017 where *in vivo* postsynaptic interactomes were isolated and analysed for changes in interaction networks in TNIK knockout mice compared to wild-type mice (Li et al., 2017). Isolation of MAGUK, DLGAP1 and SHANK3 complexes (as a readout for distribution of proteins across the three PSD layers mentioned in the introduction) from adult (12-16 weeks old) mouse brain revealed significantly reduced protein content in PSDs of TNIK knockout mice compared to the wild type. In isolated MAGUK complexes, protein content of SHANK2, SHANK3, SYNGAP1 and interestingly CNK2 was reduced. DLGAP1 complexes revealed a decreased amount for SHANK3, GRIN2a, SYNGAP1 and again CNK2 in the TNIK knockout. This is interesting, and supports especially the idea that there is a functional interplay between CNK2 and TNIK. Future studies could explore the interdependency of TNIK and CNK2 and the influence TNIK might have on CNK2 in greater depth.

4.2.1 TNIK regulation of the actin cytoskeleton

A very robust and highly reproducible effect of active TNIK is kinase-dependent cell rounding in mammalian cells by regulating actin dynamics (Fu et al., 1999; Taira et al., 2004; Wang et al., 2011a). Expression of active TNIK induces cell rounding, which is not the case following expression of the kinase dead TNIK mutant TNIK-K54R (Wang et al., 2016; Wang et al., 2011a). The effect can be completely reversed by treatment with a specific TNIK inhibitor (Wang et al., 2016). TNIK phosphorylates the actin fragmenting protein Gelsolin and induces disruption of F-actin structure, which inhibits cell spreading (Fu et al., 1999). Another TNIK substrate is the protein FMNL2, a member of the Formin family, which is associated with mental retardation (Wang et al., 2016). FMNL2 is able to polymerise straight actin filaments at the barbed ends and was shown to be involved in regulation of actin dynamics and cell morphology (Wang et al., 2016). Evidence that TNIK is important for dendritic arborisation as well as spine formation (Hussain et al., 2010; Kawabe et al., 2010) reveal its important role in regulation of the cytoskeleton of neurons.

4.2.2 TNIK phosphorylates synaptic proteins

In a study from 2016, a phosphorylation consensus sequence among TNIK substrates was identified. Interestingly, many of these proteins are associated with psychiatric or neurological disorders. The identified TNIK substrates included members of the delta-catenin family p120-catenin and delta-catenin, which are linked to autism and schizophrenia (Wang et al., 2016). Both of these catenins interact with cadherins at synapses, and multiple studies demonstrate that their regulation is an important factor in modulating dendritic spine architecture and dynamics (Brigidi and Bamji, 2011; Brigidi et al., 2014; Elia et al., 2006; Matter et al., 2009; Yuan et al., 2015). Further, signalling molecules as well as actin modulators were identified as neuronal TNIK substrates. For an overview of recently identified neuronal TNIK targets, see **Fig. 20**.
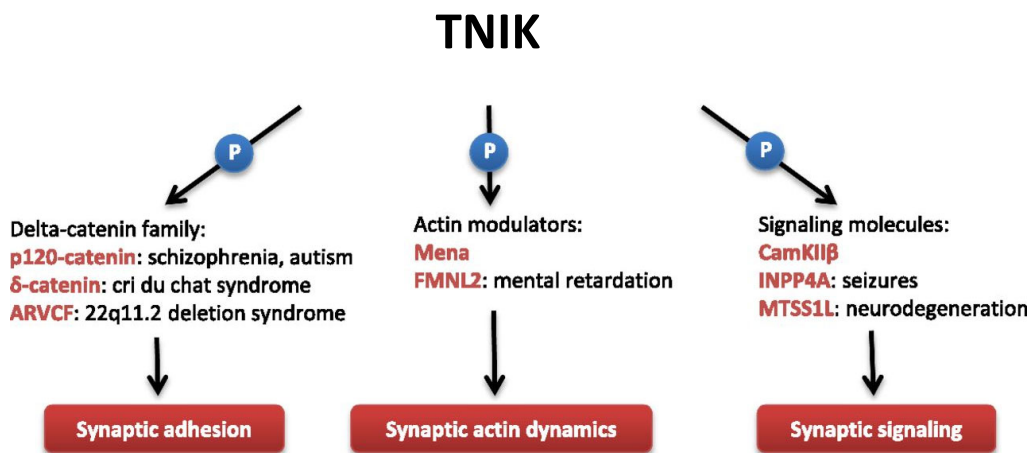
Figure 20: TNIK phosphorylates synaptic proteins

Scheme modified from Wang et al, 2016, illustrating TNIK substrates, their function and implication in neurological disease

When the consensus sequence of TNIK targets was published, we checked if this specific sequence is present in CNK2 and identified the consensus sequence T-L-P-R referring to CNK2 amino acids 846-849 as a putative TNIK target site within CNK2 **(see Fig. 21)**. It is interesting that the putative TNIK target sequence we detected in CNK2 included a

validated phosphorylation site at position T846 that was identified in a study on activity-dependent changes in phosphorylation in mouse synaptosomal preparations (Munton et al., 2007).

Figure 21: Scheme illustrating the putative TNIK consensus sequence within CNK2

Putative TNIK consensus sequence is highlighted in magenta; it refers to amino acids 846-849 within CNK2

The study from Li et al. in 2017 showed a reduction of CNK2 protein content in TNIK knockout mice compared to the wild type. This result, together with the idea that CNK2 is a putative TNIK substrate, highlights the possibility that TNIK potentially influences CNK2 expression levels by modulating phosphorylation status.

In addition, TNIK is an important regulator of JNK signalling (Fu et al., 1999; Larhammar et al., 2017; Shkoda et al., 2012), which may also have implications for regulating synaptic protein content. Previous studies have demonstrated that TNIK can activate JNK in heterologous systems and regulate JNK-dependent phosphorylation of c-jun in neurons (Dan et al., 2001; Taira et al., 2004; Zhu et al., 2005). It has also been shown that JNK-mediated phosphorylation of PSD-95 caused its accumulation in the PSD, whereas JNK-mediated phosphorylation of delta-catenin resulted in its proteasomal degradation (Kim et al., 2007; Mao and Wang, 2016). It is thus plausible that alterations in synaptic TNIK expression levels or activity might contribute to changes in the expression of multiple other synaptic proteins via regulation of JNK, and in this way regulate dendritic spine architecture. It is worth mentioning here that JNK3 is associated with intellectual disability (Kunde et al., 2013; Shoichet et al., 2006) and that JNK1 was shown to play an important role in dendritic arborization (Komulainen et al., 2014).

4.2.3 TNIK and MINK1 regulate AMPARs

Another very interesting finding is that MINK1 and TNIK are involved in regulation of surface expression of AMPA receptors (Hussain et al., 2010; Wang et al., 2011a). It was shown *e.g.* that loss of MINK1 and TNIK in neurons resulted in reduced surface expression of the AMPA receptor subunit GluR1 and AMPAR-mediated amplitude of mEPSCs was decreased upon TNIK knockdown (Hussain et al., 2010). A study from 2005 suggested that AMPAR removal during depotentiation was mediated via TNIK upon NMDAR activity (Zhu et al., 2005). Here they showed that activity of the NR2A subunit activated the GTPase Rap2, which is an effector of TNIK. Upon activation, TNIK specifically stimulates JNK signalling, which controls synaptic removal of AMPARs during depotentiation.

4.3 The interplay of CNK2 and TNIK might be important for neural development

From our studies described here and earlier studies by other groups, we know that CNK2 has multiple interaction partners and is involved in various signalling pathways, including *e. g.* protein kinase pathways like the MAPK cascade or GTPase cycling. With MINK1, TNIK, JNK1 and JNK3, four novel interaction partners were identified in this study. Interestingly, two of the novel CNK2 interaction partners identified in this study - TNIK and JNK3 - are associated with intellectual disability (Anazi et al., 2016; Kunde et al., 2013; Shoichet et al., 2006).

As CNK2 interacts with both TNIK and JNK, and TNIK activates JNK, we have reason to believe that CNK2 plays a role in the regulation of the MAPK signalling pathway involving TNIK and JNK. Data showing that CNK and KSR scaffold proteins coordinate MAPK signalling pathways, support the idea that loss or mis-function of CNK2 might result in mis-regulation of the MAPK cascade. From this study and previously published work, there is evidence that CNK2 plays an important role in membrane localisation of its interaction partners. Distinct localisation of catalytically active proteins can be crucial

for regulation of their activity. It is likely that CNK2 is involved in the activity state and the interplay of TNIK and JNK. Further studies will be needed to explore this idea.

Combining our data with the results of various other studies, we can speculate that CNK2 regulates TNIK localisation and activity. If truncated CNK2 is not able to attach to the membrane in dendritic spines, TNIK is bound but not transported to its destination, *i.e.* the normal function of the kinase TNIK is potentially blocked by its interaction with a membrane-deficient CNK2. This hypothesis is supported by the effect on PSD cluster size and spine density: Neurons expressing CNK2-ΔPH show a tendency towards reduced spine density and significantly reduced PSD size, which is in line with reports about reduction in PSD protein cluster size and number upon inhibition or of loss of TNIK (Wang et al., 2011a).

For the disease-associated CNK2 variant (EGFP-CNK2-P1), we see an accumulation of mutant protein in dendritic spines of neurons. As active TNIK was shown to protect PSD proteins, including *e. g.* GluR1, GluR2/3, PSD-95, NR2B and Stargazin from degradation (Wang et al., 2011a), a CNK2-mediated accumulation of TNIK might cause an increase in PSD protein levels. We have not tested yet if TNIK protein levels are increased in dendritic spines of neurons expressing CNK2-P1. However, it would not be surprising, as we expect an interaction between CNK2-P1 and TNIK based on our mapping the TNIK binding region of CNK2. This hypothesis is supported by the patch clamp experiments conducted in this study where we see an increase in mEPSC amplitude in neurons expressing CNK2-P1, as previous studies show that loss of TNIK results in a decrease of mEPSC amplitude (Hussain et al., 2010; Wang et al., 2011a). It is possible that the effect TNIK has on protein levels in the PSD (and especially on AMPA receptors) depends, at least in part, on its CNK2-mediated localisation. Future studies will be necessary to explore whether expression of the disease-associated CNK2-P1 variant influences protein levels of the kinase TNIK. Another question that remains unanswered is whether or not mEPSC amplitude is also affected in neurons in which TNIK is mislocalised due to interactions withCNK2-ΔPH.

Given that studies in humans and mice highlight a role for CNK2 and TNIK in related disorders, combined with the fact that diverse studies demonstrate that TNIK plays an established role in neuronal differentiation and network formation, we propose that this novel CNK2 binding partner might work in concert with CNK2 during normal neural development. We could not measure significant changes in TNIK synaptic expressionlevels upon knockdown of CNK2, which suggests that other interaction partners of TNIK may compensate for the early loss of CNK2. However, our studies indeed highlight a functional interdependence of these two proteins with regard to membrane trafficking and thereby illuminate a putative regulatory cascade that may underlie the defects responsible for the observed cognitive dysfunction in patients with CNK2 alterations. Given their physical interaction, it is also plausible that TNIK regulatory activity may be influenced by CNK2 and vice versa. Finally, it is important to note that while we focus here on the CNK2-interacting proteins of the TNIK/MINK1 family, it is likely that several other regulatory proteins are also affected by disease-associated changes in CNK2 expression. Future studies aim to explore in greater depth how diverse CNK2-mediated signal cascades participate in the cellular processes that govern neurotransmission and proper network formation.

4.4 Outlook

There are still many open questions about the function of CNK2. In future studies, we would like to address these questions on the role of CNK2 - and especially the novel link to TNIK - in greater depth. Also, of interest are the disease-associated CNK2 variants which influence spine morphology and synaptic transmission in primary hippocampal neuron cultures. Deciphering the molecular mechanisms that underly these changes is important for our understanding of CNK2-associated disease. In this section I will outline several strategies for exploring these ideas.

4.4.1 Functional link of CNK2 and TNIK

We and others have observed that overexpression of TNIK causes a cell-rounding phenotype. We aim to explore the idea that CNK2 might influence this robust effect of TNIK. Our hypothesis, based on preliminary experimental data, is that coexpression of CNK2 with TNIK in heterologous cells might reduce TNIK-mediated cell rounding. We will investigate this idea by assessing the effects of CNK2 in a TNIK-mediated cell rounding assay in HEK293T cells; for comparison we will examine the effects of other scaffold proteins, *e. g.* CNK1, which is very similar to CNK2 concerning the domain structure but does not bind TNIK (as we have shown in coIP experiments). The extent of cell rounding could be quantitatively analysed by measuring the projected cell area (Wang et al., 2016) or the ratio of cell length to breadth (Wang et al., 2011a). CNK2-mediated alterations in TNIK-regulated cell morphology changes would support our hypothesis that CNK2 in fact influences TNIK function in addition to affecting TNIK localisation. We could also take advantage of an shRNA-mediated knock down of TNIK and subsequently compare effects of CNK knockdown and TNIK knockdown on neuron and spine morphology. If we observe similar effects, this would support our hypothesis that these two proteins function together in regulatory processes that dictate spine growth and maintenance.

4.4.2 Functional link to TNIK targets

To further explore functional links between CNK2 and TNIK, we would also address the idea that the phosphorylation of TNIK substrates might be influenced by CNK2. Several neuronal TNIK targets were identified recently (Wang et al., 2016), and their phosphorylation status could be a good functional readout for TNIK activity. A very straight-forward approach would be to coexpress TNIK with either CNK2 or CNK2 variants in heterologous cells or neurons and use phospho-specific antibodies (*e. g.* phospho-JNK or phospho-catenin antibodies) to detect changes in phosphorylation of TNIK targets by western blot. In the absence of such phospho-specific antibodies, we could also take advantage of PhosTAG approaches, or pan phospho-serine or phospho-

threonine antibodies, both of which enable visualisation of the comparative phosphorylation status of target proteins in western blot assays.

4.4.3 Disease-associated CNK2 variants

It is also of particular interest and disease-relevance to determine which protein interactions are abolished by the premature termination of the disease-associated CNK2 variants. We have already observed that truncation of CNK2 affects the dynamics of the protein and influences spine morphology, but it is still not clear what happens at the molecular level. To explore which interactions are affected by truncation, we could conduct a comparative screen (with wild-type CNK2 and a disease-associated truncated CNK2) for interaction partners, *e. g.* via yeast-two-hybrid as we have done for the wild-type already. With this approach we would compare the proteins with regard to direct protein interactions. Another strategy is to take advantage of a quantitative comparative mass spectrometry approach following pulldown of selected GST-tagged CNK2 variants (again wild-type versus disease-associated) and isolation of interacting proteins from brain or crude synaptosome lysates. This strategy would allow us to examine also indirect interactions and may shed light on if and how mutant CNK2 proteins influence protein complex formation at synaptic sites.

5. References

Anazi, S., Shamseldin, H.E., AlNaqeb, D., Abouelhoda, M., Monies, D., Salih, M.A., Al-Rubeaan, K., and Alkuraya, F.S. (2016). A null mutation in TNIK defines a novel locus for intellectual disability. Hum Genet *135*, 773-778.

Aypar, U., Wirrell, E.C., and Hoppman, N.L. (2015). CNKSR2 deletions: a novel cause of X-linked intellectual disability and seizures. American journal of medical genetics Part A *167*, 1668-1670.

Baltussen, L.L., Rosianu, F., and Ultanir, S.K. (2018). Kinases in synaptic development and neurological diseases. Prog Neuropsychopharmacol Biol Psychiatry *84*, 343-352.

Bayes, A., van de Lagemaat, L.N., Collins, M.O., Croning, M.D., Whittle, I.R., Choudhary, J.S., and Grant, S.G. (2011). Characterization of the proteome, diseases and evolution of the human postsynaptic density. Nat Neurosci *14*, 19-21.

Boccuto, L., Lauri, M., Sarasua, S.M., Skinner, C.D., Buccella, D., Dwivedi, A., Orteschi, D., Collins, J.S., Zollino, M., Visconti, P.*, et al.* (2013). Prevalence of SHANK3 variants in patients with different subtypes of autism spectrum disorders. Eur J Hum Genet *21*, 310-316.

Brigidi, G.S., and Bamji, S.X. (2011). Cadherin-catenin adhesion complexes at the synapse. Curr Opin Neurobiol *21*, 208-214.

Brigidi, G.S., Sun, Y., Beccano-Kelly, D., Pitman, K., Mobasser, M., Borgland, S.L., Milnerwood, A.J., and Bamji, S.X. (2014). Palmitoylation of delta-catenin by DHHC5 mediates activity-induced synapse plasticity. Nat Neurosci *17*, 522-532.

Bumeister, R., Rosse, C., Anselmo, A., Camonis, J., and White, M.A. (2004). CNK2 couples NGF signal propagation to multiple regulatory cascades driving cell differentiation. Current biology : CB *14*, 439-445.

Burette, A.C., Phend, K.D., Burette, S., Lin, Q.C., Liang, M.S., Foltz, G., Taylor, N., Wang, Q., Brandon, N.J., Bates, B.*, et al.* (2015). Organization of TNIK in dendritic spines. J Comp Neurol *523*, 1913-1924.

Chen, H., Tang, A.H., and Blanpied, T.A. (2018). Subsynaptic spatial organization as a regulator of synaptic strength and plasticity. Curr Opin Neurobiol *51*, 147-153.

Cho, H.J., Hwang, Y.S., Mood, K., Ji, Y.J., Lim, J., Morrison, D.K., and Daar, I.O. (2014). EphrinB1 interacts with CNK1 and promotes cell migration through c-Jun N-terminal kinase (JNK) activation. J Biol Chem *289*, 18556-18568.

Choquet, D., and Triller, A. (2013). The dynamic synapse. Neuron *80*, 691-703.

Ciocanel, M.V., Kreiling, J.A., Gagnon, J.A., Mowry, K.L., and Sandstede, B. (2017). Analysis of Active Transport by Fluorescence Recovery after Photobleaching. Biophys J *112*, 1714-1725.

Claperon, A., and Therrien, M. (2007). KSR and CNK: two scaffolds regulating RAS-mediated RAF activation. Oncogene *26*, 3143-3158.

Coba, M.P., Komiyama, N.H., Nithianantharajah, J., Kopanitsa, M.V., Indersmitten, T., Skene, N.G., Tuck, E.J., Fricker, D.G., Elsegood, K.A., Stanford, L.E.*, et al.* (2012). TNiK is required for

postsynaptic and nuclear signaling pathways and cognitive function. J Neurosci *32*, 13987-13999.

Collins, M.O., Husi, H., Yu, L., Brandon, J.M., Anderson, C.N., Blackstock, W.P., Choudhary, J.S., and Grant, S.G. (2006). Molecular characterization and comparison of the components and multiprotein complexes in the postsynaptic proteome. J Neurochem *97 Suppl 1*, 16-23.

Damiano, J.A., Burgess, R., Kivity, S., Lerman-Sagie, T., Afawi, Z., Scheffer, I.E., Berkovic, S.F., and Hildebrand, M.S. (2017). Frequency of CNKSR2 mutation in the X-linked epilepsy-aphasia spectrum. Epilepsia *58*, E40-E43.

Dan, I., Watanabe, N.M., and Kusumi, A. (2001). The Ste20 group kinases as regulators of MAP kinase cascades. Trends Cell Biol *11*, 220-230.

de Bartolomeis, A., Latte, G., Tomasetti, C., and Iasevoli, F. (2014). Glutamatergic postsynaptic density protein dysfunctions in synaptic plasticity and dendritic spines morphology: relevance to schizophrenia and other behavioral disorders pathophysiology, and implications for novel therapeutic approaches. Mol Neurobiol *49*, 484-511.

Douziech, M., Roy, F., Laberge, G., Lefrancois, M., Armengod, A.V., and Therrien, M. (2003). Bimodal regulation of RAF by CNK in Drosophila. EMBO J *22*, 5068-5078.

Durand, C.M., Betancur, C., Boeckers, T.M., Bockmann, J., Chaste, P., Fauchereau, F., Nygren, G., Rastam, M., Gillberg, I.C., Anckarsater, H.*, et al.* (2007). Mutations in the gene encoding the synaptic scaffolding protein SHANK3 are associated with autism spectrum disorders. Nat Genet *39*, 25-27.

Elia, L.P., Yamamoto, M., Zang, K., and Reichardt, L.F. (2006). p120 catenin regulates dendritic spine and synapse development through Rho-family GTPases and cadherins. Neuron *51*, 43-56.

Fernandez, E., Collins, M.O., Uren, R.T., Kopanitsa, M.V., Komiyama, N.H., Croning, M.D., Zografos, L., Armstrong, J.D., Choudhary, J.S., and Grant, S.G. (2009). Targeted tandem affinity purification of PSD-95 recovers core postsynaptic complexes and schizophrenia susceptibility proteins. Mol Syst Biol *5*, 269.

Fischer, A., Muhlhauser, W.W.D., Warscheid, B., and Radziwill, G. (2017). Membrane localization of acetylated CNK1 mediates a positive feedback on RAF/ERK signaling. Sci Adv *3*, e1700475.

Frank, R.A., and Grant, S.G. (2017). Supramolecular organization of NMDA receptors and the postsynaptic density. Curr Opin Neurobiol *45*, 139-147.

Fritz, R.D., Varga, Z., and Radziwill, G. (2010). CNK1 is a novel Akt interaction partner that promotes cell proliferation through the Akt-FoxO signalling axis. Oncogene *29*, 3575-3582.

Fu, C.A., Shen, M., Huang, B.C., Lasaga, J., Payan, D.G., and Luo, Y. (1999). TNIK, a novel member of the germinal center kinase family that activates the c-Jun N-terminal kinase pathway and regulates the cytoskeleton. J Biol Chem *274*, 30729-30737.

Good, M.C., Zalatan, J.G., and Lim, W.A. (2011). Scaffold proteins: hubs for controlling the flow of cellular information. Science *332*, 680-686.

Goodman, L., Baddeley, D., Ambroziak, W., Waites, C.L., Garner, C.C., Soeller, C., and Montgomery, J.M. (2017). N-terminal SAP97 isoforms differentially regulate synaptic structure and postsynaptic surface pools of AMPA receptors. Hippocampus *27*, 668-682.

Gray, E.G. (1959). Axo-somatic and axo-dendritic synapses of the cerebral cortex: an electron microscope study. J Anat *93*, 420-433.

Guang, S., Pang, N., Deng, X., Yang, L., He, F., Wu, L., Chen, C., Yin, F., and Peng, J. (2018). Synaptopathology Involved in Autism Spectrum Disorder. Front Cell Neurosci *12*, 470.

Ha, H.T.T., Leal-Ortiz, S., Lalwani, K., Kiyonaka, S., Hamachi, I., Mysore, S.P., Montgomery, J.M., Garner, C.C., Huguenard, J.R., and Kim, S.A. (2018). Shank and Zinc Mediate an AMPA Receptor Subunit Switch in Developing Neurons. Front Mol Neurosci *11*, 405.

Herculano-Houzel, S. (2009). The human brain in numbers: a linearly scaled-up primate brain. Front Hum Neurosci *3*, 31.

Houge, G., Rasmussen, I.H., and Hovland, R. (2012). Loss-of-Function CNKSR2 Mutation Is a Likely Cause of Non-Syndromic X-Linked Intellectual Disability. Molecular syndromology *2*, 60-63.

Hu, H., Haas, S.A., Chelly, J., Van Esch, H., Raynaud, M., de Brouwer, A.P., Weinert, S., Froyen, G., Frints, S.G., Laumonnier, F.*, et al.* (2016). X-exome sequencing of 405 unresolved families identifies seven novel intellectual disability genes. Molecular psychiatry *21*, 133-148.

Hung, A.Y., Futai, K., Sala, C., Valtschanoff, J.G., Ryu, J., Woodworth, M.A., Kidd, F.L., Sung, C.C., Miyakawa, T., Bear, M.F.*, et al.* (2008). Smaller dendritic spines, weaker synaptic transmission, but enhanced spatial learning in mice lacking Shank1. J Neurosci *28*, 1697-1708.

Hussain, N.K., Hsin, H., Huganir, R.L., and Sheng, M. (2010). MINK and TNIK differentially act on Rap2-mediated signal transduction to regulate neuronal structure and AMPA receptor function. J Neurosci *30*, 14786-14794.

Iasevoli, F., Tomasetti, C., and de Bartolomeis, A. (2013). Scaffolding proteins of the post-synaptic density contribute to synaptic plasticity by regulating receptor localization and distribution: relevance for neuropsychiatric diseases. Neurochem Res *38*, 1-22.

Iida, J., Nishimura, W., Yao, I., and Hata, Y. (2002). Synaptic localization of membrane-associated guanylate kinase-interacting protein mediated by the pleckstrin homology domain. Eur J Neurosci *15*, 1493-1498.

Jaffe, A.B., Aspenstrom, P., and Hall, A. (2004). Human CNK1 acts as a scaffold protein, linking Rho and Ras signal transduction pathways. Mol Cell Biol *24*, 1736-1746.

Jaffe, A.B., Hall, A., and Schmidt, A. (2005). Association of CNK1 with Rho guanine nucleotide exchange factors controls signaling specificity downstream of Rho. Current biology : CB *15*, 405-412.

Kawabe, H., Neeb, A., Dimova, K., Young, S.M., Jr., Takeda, M., Katsurabayashi, S., Mitkovski, M., Malakhova, O.A., Zhang, D.E., Umikawa, M.*, et al.* (2010). Regulation of Rap2A by the ubiquitin ligase Nedd4-1 controls neurite development. Neuron *65*, 358-372.

Kim, E., Naisbitt, S., Hsueh, Y.P., Rao, A., Rothschild, A., Craig, A.M., and Sheng, M. (1997). GKAP, a novel synaptic protein that interacts with the guanylate kinase-like domain of the PSD-95/SAP90 family of channel clustering molecules. J Cell Biol *136*, 669-678.

Kim, E., and Sheng, M. (2004). PDZ domain proteins of synapses. Nat Rev Neurosci *5*, 771-781.

Kim, M.J., Futai, K., Jo, J., Hayashi, Y., Cho, K., and Sheng, M. (2007). Synaptic accumulation of PSD-95 and synaptic function regulated by phosphorylation of serine-295 of PSD-95. Neuron *56*, 488-502.

Komulainen, E., Zdrojewska, J., Freemantle, E., Mohammad, H., Kulesskaya, N., Deshpande, P., Marchisella, F., Mysore, R., Hollos, P., Michelsen, K.A.*, et al.* (2014). JNK1 controls dendritic field size in L2/3 and L5 of the motor cortex, constrains soma size, and influences fine motor coordination. Front Cell Neurosci *8*, 272.

Kunde, S.A., Rademacher, N., Tzschach, A., Wiedersberg, E., Ullmann, R., Kalscheuer, V.M., and Shoichet, S.A. (2013). Characterisation of de novo MAPK10/JNK3 truncation mutations associated with cognitive disorders in two unrelated patients. Hum Genet *132*, 461-471.

Lanigan, T.M., Liu, A., Huang, Y.Z., Mei, L., Margolis, B., and Guan, K.L. (2003). Human homologue of Drosophila CNK interacts with Ras effector proteins Raf and Rlf. FASEB J *17*, 2048-2060.

Larhammar, M., Huntwork-Rodriguez, S., Rudhard, Y., Sengupta-Ghosh, A., and Lewcock, J.W. (2017). The Ste20 Family Kinases MAP4K4, MINK1, and TNIK Converge to Regulate Stress-Induced JNK Signaling in Neurons. J Neurosci *37*, 11074-11084.

Laumonnier, F., Cuthbert, P.C., and Grant, S.G. (2007). The role of neuronal complexes in human X-linked brain diseases. Am J Hum Genet *80*, 205-220.

Lemmon, M.A. (2008). Membrane recognition by phospholipid-binding domains. Nat Rev Mol Cell Biol *9*, 99-111.

Li, J., Zhang, W., Yang, H., Howrigan, D.P., Wilkinson, B., Souaiaia, T., Evgrafov, O.V., Genovese, G., Clementel, V.A., Tudor, J.C.*, et al.* (2017). Spatiotemporal profile of postsynaptic interactomes integrates components of complex brain disorders. Nat Neurosci *20*, 1150-1161.

Lim, J., Ritt, D.A., Zhou, M., and Morrison, D.K. (2014). The CNK2 scaffold interacts with vilse and modulates Rac cycling during spine morphogenesis in hippocampal neurons. Current biology : CB *24*, 786-792.

Lim, J., Zhou, M., Veenstra, T.D., and Morrison, D.K. (2010). The CNK1 scaffold binds cytohesins and promotes insulin pathway signaling. Genes Dev *24*, 1496-1506.

Lippincott-Schwartz, J., Snapp, E.L., and Phair, R.D. (2018). The Development and Enhancement of FRAP as a Key Tool for Investigating Protein Dynamics. Biophys J *115*, 1146-1155.
Lois, C., Hong, E.J., Pease, S., Brown, E.J., and Baltimore, D. (2002). Germline transmission and tissue-specific expression of transgenes delivered by lentiviral vectors. Science *295*, 868-872.

Macias, M.J., Wiesner, S., and Sudol, M. (2002). WW and SH3 domains, two different scaffolds to recognize proline-rich ligands. FEBS Lett *513*, 30-37.

MacLaren, E.J., Charlesworth, P., Coba, M.P., and Grant, S.G. (2011). Knockdown of mental disorder susceptibility genes disrupts neuronal network physiology in vitro. Mol Cell Neurosci *47*, 93-99.

Mao, L.M., and Wang, J.Q. (2016). Synaptically Localized Mitogen-Activated Protein Kinases: Local Substrates and Regulation. Mol Neurobiol *53*, 6309-6315.

Matter, C., Pribadi, M., Liu, X., and Trachtenberg, J.T. (2009). Delta-catenin is required for the maintenance of neural structure and function in mature cortex in vivo. Neuron *64*, 320-327.

Meyer, D., Bonhoeffer, T., and Scheuss, V. (2014). Balance and stability of synaptic structures during synaptic plasticity. Neuron *82*, 430-443.

Moessner, R., Marshall, C.R., Sutcliffe, J.S., Skaug, J., Pinto, D., Vincent, J., Zwaigenbaum, L., Fernandez, B., Roberts, W., Szatmari, P*., et al.* (2007). Contribution of SHANK3 mutations to autism spectrum disorder. Am J Hum Genet *81*, 1289-1297.

Monteiro, P., and Feng, G. (2017). SHANK proteins: roles at the synapse and in autism spectrum disorder. Nat Rev Neurosci *18*, 147-157.

Morrison, D.K., and Davis, R.J. (2003). Regulation of MAP kinase signaling modules by scaffold proteins in mammals. Annu Rev Cell Dev Biol *19*, 91-118.

Munton, R.P., Tweedie-Cullen, R., Livingstone-Zatchej, M., Weinandy, F., Waidelich, M., Longo, D., Gehrig, P., Potthast, F., Rutishauser, D., Gerrits, B*., et al.* (2007). Qualitative and quantitative analyses of protein phosphorylation in naive and stimulated mouse synaptosomal preparations. Mol Cell Proteomics *6*, 283-293.

Naisbitt, S., Kim, E., Tu, J.C., Xiao, B., Sala, C., Valtschanoff, J., Weinberg, R.J., Worley, P.F., and Sheng, M. (1999). Shank, a novel family of postsynaptic density proteins that binds to the NMDA receptor/PSD-95/GKAP complex and cortactin. Neuron *23*, 569-582.

Najmabadi, H., Hu, H., Garshasbi, M., Zemojtel, T., Abedini, S.S., Chen, W., Hosseini, M., Behjati, F., Haas, S., Jamali, P*., et al.* (2011). Deep sequencing reveals 50 novel genes for recessive cognitive disorders. Nature *478*, 57-63.

Nwabuisi-Heath, E., LaDu, M.J., and Yu, C. (2012). Simultaneous analysis of dendritic spine density, morphology and excitatory glutamate receptors during neuron maturation in vitro by quantitative immunocytochemistry. J Neurosci Methods *207*, 137-147.

Ohtakara, K., Nishizawa, M., Izawa, I., Hata, Y., Matsushima, S., Taki, W., Inada, H., Takai, Y., and Inagaki, M. (2002). Densin-180, a synaptic protein, links to PSD-95 through its direct interaction with MAGUIN-1. Genes Cells *7*, 1149-1160.

Peca, J., Feliciano, C., Ting, J.T., Wang, W., Wells, M.F., Venkatraman, T.N., Lascola, C.D., Fu, Z., and Feng, G. (2011). Shank3 mutant mice display autistic-like behaviours and striatal dysfunction. Nature *472*, 437-442.

Qiao, F., and Bowie, J.U. (2005). The many faces of SAM. Sci STKE *2005*, re7.

Rocheleau, C.E., Ronnlund, A., Tuck, S., and Sundaram, M.V. (2005). Caenorhabditis elegans CNK-1 promotes Raf activation but is not essential for Ras/Raf signaling. Proc Natl Acad Sci U S A *102*, 11757-11762.

Ropers, H.H., and Hamel, B.C. (2005). X-linked mental retardation. Nat Rev Genet *6*, 46-57.

Sala, C., Futai, K., Yamamoto, K., Worley, P.F., Hayashi, Y., and Sheng, M. (2003). Inhibition of dendritic spine morphogenesis and synaptic transmission by activity-inducible protein Homer1a. J Neurosci *23*, 6327-6337.

Sala, C., Piech, V., Wilson, N.R., Passafaro, M., Liu, G., and Sheng, M. (2001). Regulation of dendritic spine morphology and synaptic function by Shank and Homer. Neuron *31*, 115-130.

Schindelin, J., Arganda-Carreras, I., Frise, E., Kaynig, V., Longair, M., Pietzsch, T., Preibisch, S., Rueden, C., Saalfeld, S., Schmid, B.*, et al.* (2012). Fiji: an open-source platform for biological-image analysis. Nat Methods *9*, 676-682.

Schoneborn, H., Raudzus, F., Coppey, M., Neumann, S., and Heumann, R. (2018). Perspectives of RAS and RHEB GTPase Signaling Pathways in Regenerating Brain Neurons. Int J Mol Sci *19*.

Sheng, M., and Kim, E. (2011). The postsynaptic organization of synapses. Cold Spring Harb Perspect Biol *3*.

Shkoda, A., Town, J.A., Griese, J., Romio, M., Sarioglu, H., Knofel, T., Giehler, F., and Kieser, A. (2012). The germinal center kinase TNIK is required for canonical NF-kappaB and JNK signaling in B-cells by the EBV oncoprotein LMP1 and the CD40 receptor. PLoS Biol *10*, e1001376.

Shoichet, S.A., Duprez, L., Hagens, O., Waetzig, V., Menzel, C., Herdegen, T., Schweiger, S., Dan, B., Vamos, E., Ropers, H.H.*, et al.* (2006). Truncation of the CNS-expressed JNK3 in a patient with a severe developmental epileptic encephalopathy. Hum Genet *118*, 559-567.

Skuse, D.H. (2005). X-linked genes and mental functioning. Hum Mol Genet *14 Spec No 1*, R27-32.

Stornetta, R.L., and Zhu, J.J. (2011). Ras and Rap signaling in synaptic plasticity and mental disorders. Neuroscientist *17*, 54-78.

Sun, Y., Liu, Y.D., Xu, Z.F., Kong, Q.X., and Wang, Y.L. (2018). CNKSR2 mutation causes the X-linked epilepsy-aphasia syndrome: A case report and review of literature. World J Clin Cases *6*, 570-576.

Szumlinski, K.K., Kalivas, P.W., and Worley, P.F. (2006). Homer proteins: implications for neuropsychiatric disorders. Curr Opin Neurobiol *16*, 251-257.

Taira, K., Umikawa, M., Takei, K., Myagmar, B.E., Shinzato, M., Machida, N., Uezato, H., Nonaka, S., and Kariya, K. (2004). The Traf2- and Nck-interacting kinase as a putative effector of Rap2 to regulate actin cytoskeleton. J Biol Chem *279*, 49488-49496.

Therrien, M., Wong, A.M., and Rubin, G.M. (1998). CNK, a RAF-binding multidomain protein required for RAS signaling. Cell *95*, 343-353.

Vaags, A.K., Bowdin, S., Smith, M.L., Gilbert-Dussardier, B., Brocke-Holmefjord, K.S., Sinopoli, K., Gilles, C., Haaland, T.B., Vincent-Delorme, C., Lagrue, E.*, et al.* (2014). Absent CNKSR2 causes seizures and intellectual, attention, and language deficits. Ann Neurol *76*, 758-764.

Veerapathiran, S., and Wohland, T. (2018). Fluorescence techniques in developmental biology. J Biosci *43*, 541-553.

Vinade, L., Chang, M., Schlief, M.L., Petersen, J.D., Reese, T.S., Tao-Cheng, J.H., and Dosemeci, A. (2003). Affinity purification of PSD-95-containing postsynaptic complexes. J Neurochem *87*, 1255-1261.

von Bartheld, C.S., Bahney, J., and Herculano-Houzel, S. (2016). The search for true numbers of neurons and glial cells in the human brain: A review of 150 years of cell counting. J Comp Neurol *524*, 3865-3895.

Wang, Q., Amato, S.P., Rubitski, D.M., Hayward, M.M., Kormos, B.L., Verhoest, P.R., Xu, L., Brandon, N.J., and Ehlers, M.D. (2016). Identification of Phosphorylation Consensus Sequences and Endogenous Neuronal Substrates of the Psychiatric Risk Kinase TNIK. J Pharmacol Exp Ther *356*, 410-423.

Wang, Q., Charych, E.I., Pulito, V.L., Lee, J.B., Graziane, N.M., Crozier, R.A., Revilla-Sanchez, R., Kelly, M.P., Dunlop, A.J., Murdoch, H.*, et al.* (2011a). The psychiatric disease risk factors DISC1 and TNIK interact to regulate synapse composition and function. Molecular psychiatry *16*, 1006-1023.

Wang, X., McCoy, P.A., Rodriguiz, R.M., Pan, Y., Je, H.S., Roberts, A.C., Kim, C.J., Berrios, J., Colvin, J.S., Bousquet-Moore, D.*, et al.* (2011b). Synaptic dysfunction and abnormal behaviors in mice lacking major isoforms of Shank3. Hum Mol Genet *20*, 3093-3108.

Watt, J.L., Olson, I.A., Johnston, A.W., Ross, H.S., Couzin, D.A., and Stephen, G.S. (1985). A familial pericentric inversion of chromosome 22 with a recombinant subject illustrating a 'pure' partial monosomy syndrome. J Med Genet *22*, 283-287.

Wennerberg, K., Rossman, K.L., and Der, C.J. (2005). The Ras superfamily at a glance. J Cell Sci *118*, 843-846.

Whisenant, T.C., Ho, D.T., Benz, R.W., Rogers, J.S., Kaake, R.M., Gordon, E.A., Huang, L., Baldi, P., and Bardwell, L. (2010). Computational prediction and experimental verification of new MAP kinase docking sites and substrates including Gli transcription factors. PLoS Comput Biol *6*.

Wolfstetter, G., Pfeifer, K., van Dijk, J.R., Hugosson, F., Lu, X., and Palmer, R.H. (2017). The scaffolding protein Cnk binds to the receptor tyrosine kinase Alk to promote visceral founder cell specification in Drosophila. Sci Signal *10*.
Yao, I., Hata, Y., Ide, N., Hirao, K., Deguchi, M., Nishioka, H., Mizoguchi, A., and Takai, Y. (1999). MAGUIN, a novel neuronal membrane-associated guanylate kinase-interacting protein. J Biol Chem *274*, 11889-11896.

Yuan, L., Seong, E., Beuscher, J.L., and Arikkath, J. (2015). delta-Catenin Regulates Spine Architecture via Cadherin and PDZ-dependent Interactions. J Biol Chem *290*, 10947-10957.

Zhu, Y., Pak, D., Qin, Y., McCormack, S.G., Kim, M.J., Baumgart, J.P., Velamoor, V., Auberson, Y.P., Osten, P., van Aelst, L.*, et al.* (2005). Rap2-JNK removes synaptic AMPA receptors during depotentiation. Neuron *46*, 905-916.

Zieger, H., Kunde, S.A., Rademacher, N., Schmerl B., Shoichet, S.A. (2019). Disease-associated scaffold protein CNK2 modulates PSD size and influences trafficking of new synaptic binding partner TNIK. bioRxiv, 532374

Ziv, N.E., and Fisher-Lavie, A. (2014). Presynaptic and postsynaptic scaffolds: dynamics fast and slow. Neuroscientist *20*, 439-452.

6. Publications

- Disease-associated scaffold protein CNK2 modulates PSD size and influences trafficking of new synaptic binding partner TNIK; Zieger H, Kunde SA, Rademacher N, Schmerl B, Shoichet SA; bioRxiv 532374; 2019

  Submitted and reviewed at scientific reports, currently under revision

Manuscripts in preparation

- Investigations into the function of disease-associated scaffold protein CNK2 in neurons; Zieger H, Kunde SA and Shoichet SA; manuscript in preparation

Poster Presentations

- FENS Berlin 2018; Investigations into disease-associated scaffold proteins in the postsynaptic density; Zieger H, Kunde SA, Shoichet SA, 2018

- EMBO Practical Course, King´s College, London; Investigations into disease-associated scaffold proteins in the postsynaptic density; Zieger H, Kunde SA, Shoichet SA, 2017

- FEBS Berlin 2015; JNK-associated scaffold proteins and their role in the development and function of neurons; Zieger H, Kunde SA, Shoichet SA; 2015

- BNF (Berlin Neuroscience Forum); Scaffold proteins involved in intellectual disability, Zieger H, Kunde SA, Shoichet SA; 2014

7. Declaration of authorship

I declare that the work presented in my thesis has been conducted independently and without inappropriate support. All sources of information are referenced. This thesis has not been submitted to this or any other university.